Applied Thermal Engineering 245 (2024) 122843

Contents lists available at ScienceDirect

Applied Thermal Engineering

journal homepage: www.elsevier.com/locate/apthermeng

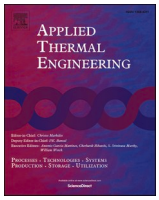

Research Paper

A methodology to reduce the computational effort in 3D-CFD simulations of plate-fin heat exchangers

Federico Torri [a,*], Fabio Berni [a], Mauro Giacalone [b], Sara Mantovani [b], Silvio Defanti [a], Giulia Colombini [a], Elena Bassoli [a], Andrea Merulla [c], Stefano Fontanesi [a]

[a] Engineering Department "Enzo Ferrari", University of Modena and Reggio Emilia, Via Vivarelli 10, 41125, Modena, Italy
[b] MilleChili Lab, Engineering Department "Enzo Ferrari", University of Modena and Reggio Emilia, Via Vivarelli 10, 41125, Modena Italy
[c] Ferrari S.p.a., Via Abetone Inf. 4, 41053 Maranello, MO, Italy

ARTICLE INFO

Keywords:
Heat Exchanger
Computational Cost
Heat Transfer
Pressure Drop
Reynolds Stress Model
CFD

ABSTRACT

The analysis of a plate-fin heat exchanger performance requires the evaluation of key parameters such as heat transfer and pressure drop. In this regard, Computational Fluid Dynamics (CFD) can be proficiently adopted, at the design stage, to predict the performance of plate-fin heat exchangers. However, these last are often characterized by a complex geometry, such as in the case of plate exchangers with turbulators, leading to a huge computational effort, which often exceeds the available resources. In this study, a numerical methodology for the simulation of plate heat exchangers is proposed, to bypass the limits imposed by the computational cost. The methodology relies on the simulation of a minimal portion of the exchanger (two plates, one per fluid) characterized by periodic boundary conditions (that mimic the presence of several layers). The total heat exchanged is obtained simply multiplying the calculated heat transfer by the number of plate couples composing the device. Moreover, the two plates allow to calibrate porous media which are adopted to rebuild (in a simplified version) the two fluid circuits of the whole exchanger and obtain the overall pressure drop across the device for both the hot and cold fluids.

The proposed approach is validated against experimental data of an oil cooler for automotive application, that is a plate-fin heat exchanger characterized by the presence of turbulators. The numerical outcomes are compared to the experiments in terms of pressure drop and heat transfer for a wide range of volumetric flow rates. Particular attention is devoted to the mesh sensitivity and the adopted computational grid minimizes the number of cells (and, thus, the computational cost), without compromising the accuracy. Moreover, the Reynolds-Stress-Transport turbulence model is accurately selected among the most diffused ones, in order to properly match the test bench data.

The proposed methodology allows to reduce of nearly one order of magnitude the total number of cells required for the simulation of the heat exchanger performance. The heat transfer is predicted with high accuracy, i.e. error is always lower than 4%. As for the pressure loss, the deviation compared to the experiments increases up to nearly 15% (for one of the simulated conditions) but it is considered still acceptable.

1. Introduction

Thermal management is of paramount importance in industrial engineering. Indeed, many applications (such as power generation and refrigeration) involve massive heat transfer, with the consequence that components and/or fluids often require a proper cooling. In this context, heat exchangers are key components. These devices can be proficiently adopted to cool fluids that are directly involved in processes (such as alimentary liquids in food industry [2]) or exploited, in turn, to cool down components suffering noticeable thermal stresses (such as blades in gas turbines). The heat transfer efficiency is the main parameter to characterize the performance of a heat exchanger. The optimization of this parameter plays a key role in terms of energy efficiency, which is of primary importance in the context of the increasingly stringent EU and USA emissions regulations [3,4].

The performance of a heat exchanger can be evaluated in terms of

* Corresponding author.
E-mail address: federico.torri@unimore.it (F. Torri).

https://doi.org/10.1016/j.applthermaleng.2024.122843
Received 24 October 2023; Received in revised form 16 February 2024; Accepted 28 February 2024
Available online 4 March 2024

pressure drop between inlet and outlet and efficiency. The lower the former is, the less the work required to force the flow through the device results. As for the latter, the greater it is, the smaller the exchanger can be. With reference to the automotive sector, smaller components simultaneously mean a reduction of weight and occupied volume, with an increase of the power-to-weight ratio and a simultaneous decrease of the design constraints. Therefore, designers usually dedicate great effort to the optimization of these components. Limiting the discussion to plate heat exchangers, which are a widely adopted solution in industry, several approaches are described in literature for their optimization. For example, the efforts of the scientific community focused on geometrical aspects and coolant properties. In particular, as for these last, the adoption of nanofluids was investigated. Zhao *et al.*[5] and Giurgiu *et al.* [6] performed a numerical comparative study between different inclination angles for a chevron corrugated plate heat exchanger, while Wang *et al.*[7] carried out a numerical analysis considering corrugation depth too. Khanlari *et al.*[8,9] presented a numerical-experimental comparison on the heat transfer performance of a plate heat exchanger using hybrid nanofluids, showing an average increase in terms of heat transfer up to 11 % compared to water. Arsenyeva *et al.* [10] provided a review of the state of the art of these optimization approaches. Nevertheless, it is evident that conducting experimental tests over a wide range of geometrical solutions or different coolants to find out an optimal solution can be prohibitively expensive both in terms of time and resources.

In this regard, 3D-CFD represents a powerful tool not only to optimize the efficiency of the devices, but also to speed up the design process, thus reducing time and cost to market. Notably, CFD analyses can be used to investigate both fluid dynamic and heat transfer aspects, especially in complex geometries associated to innovative heat exchangers. The latter can be compared to more traditional configurations in order to select the optimum [11,12]. Hayat *et al.*[13] provided a detailed overview of examples of CFD applications in the study and design optimization of heat exchangers. However, despite the benefits, a well-known limit associated with the 3D-CFD application is the large computational cost required to obtain accurate results. Moreover, the persistent push towards the maximization of the efficiency and the miniaturization of the components leads to the adoption of increasingly complicated structures [14], which makes the numerical simulation even harder in terms of computational effort. Therefore, different methodologies were developed in the past, with the aim of overcoming the limits fixed by computational costs.

Some authors relied on the simulation of a subsystem of the overall geometry, yielding correlations for Nusselt number and friction factor. For example, the core portion of a single plate can be used to predict the behavior of the whole exchanger (multiplate device). Sarraf *et al.*[15] exploited such approach on a corrugated profile of a brazed plate heat exchanger. Similarly, Ranganayakulu *et al.*[16] applied the aforementioned approach to offset and wavy fins compact heat exchangers and they were able to estimate the pressure drop with an error of 20 %. Even though this approach may be convenient in terms of computational effort, it does not consider the uneven plate-to-plate distribution of the flow and the concentrated losses at inlets and outlets.

Other methodologies rely on porous media to model heat exchangers, keeping thermal and flow characteristics and simultaneously reducing the numerical burden. The porous model can be fed directly with experimental data and used to predict the behaviour of the exchanger. Such an approach was already applied in 1972 by Spalding *et al.* [17]. Afterwards, Missirlis *et al.* [18,19]exploited a porous medium to model the flow field in an elliptical-tube heat exchanger intended to recover the thermal energy from the exhaust gas of an aero-engine. Musto *et al.* [20] utilized the same approach to model an oil cooler for aerospace applications, estimating the pressure drop and imposing the heat transfer via experimental evidence. The proposed simplified approach was validated by comparing the numerical results with the experimental counterparts.

As an alternative to the experimental data, the porous model can be fed with data from CFD simulations of the actual geometry. Cardoso *et al.* [21] applied a porous-medium-based approach to describe the fluid dynamic behavior of the flow inside a compact heat exchanger with mini channels and they were able to match the experimental measurements of pressure drop within a 2 % of error. Similarly, Wang *et al.* [22]applied the porous-medium-based approach to describe the pressure drop associated with a plate-fin heat exchanger. Other examples of pressure drop estimation via porous media are [23,24,25,26,27]. More in detail, in [23], Qu *et al.* characterized the pressure drop associated to a finned elliptic tube heat exchanger with a maximum deviation of 10 % with respect to the experimental data. The model was tested for flows with Reynolds numbers between 2000 and 12000. Similarly, Li *et al.*[24] modelled a finned elliptic tube heat exchanger working at Reynolds numbers between 4000 and 10000. Even in this case, the model showed an acceptable error (12 %) when compared to the experiments. Both in [23] and [24], a small periodic element of the actual geometry was simulated to obtain a relation between pressure drop and flow velocity, which was then provided to the porous model. Moreover, in [26], Du *et al.* applied this methodology to successfully characterize the pressure drop of a plate heat exchanger with staggered offset fins. More complex approaches were adopted by Della Torre *et al.* [25], and Yuan *et al.* [27], to estimate not only pressure drop but also heat transfer. In particular, Della Torre *et al.* [25] modelled two separate porous regions characterized by momentum and energy source terms to provide pressure drop and heat transfer estimations. Instead, Yuan *et al.* [27] exploited a 0-D model which relies on two porous regions coexisting in the same domain and sharing the same mesh. In this model, the fluid dynamic solution of the two fluids is decoupled, while a local heat transfer coefficient is associated to each cell as a function of the velocity of the two fluids in the cell itself, thus allowing the a local heat transfer estimation.

Based on the literature review, there are two main categories of works. In the first one, experimental data are adopted to calibrate the porous medium and, thus, the proposed methodologies are not predictive at all. In the second one, there are approaches based on the simulation of the actual geometry on a small scale, i.e. the analysis is limited to a Representative Elementary Volume (REV [25]). This strategy is also widely adopted in the structural simulation of periodic structures [28], which are increasingly adopted in the design of additively manufactured parts [29]. The REV approach is exploited (instead of experiments) to calibrate the coefficients of the porous medium, which is adopted, in turn, to model the whole heat exchanger. In this case, the approach can be fully predictive but at the expense of a long and careful tuning procedure. In fact, as widely discussed in [25], it is necessary to simulate the REV at different mass flow rates to obtain the pressure drop curve (from which the porous medium coefficients are extrapolated) as a function of the flow velocity. Moreover, in the case of orthotropic behavior, different flow directions have to be accounted for. Finally, REV based methodologies are even more complex, from both a modeling and implementation standpoint, if they target heat transfer too.

In the light of this, the present paper proposes a 3D-CFD methodology to predict pressure drop and heat transfer in conventional plate-fin heat exchangers [1]. The methodology aims at reducing the computational cost associated to numerical analyses of a whole exchanger simultaneously limiting both the tedious calibration and the non-trivial implementation characterizing the existing approaches available in literature. For this purpose, similarly to the literature examples, the methodology relies on a porous medium. However, compared to the available publications, the calibration of the porous medium coefficients to provide proper pressure drop and heat transfer is not carried out based on data provided by REV simulations. Instead, it is performed against a reduced version of the original heat exchanger, based on just two plates and characterized by periodic boundary conditions to mimic the presence of the other layers. Once the porous media of the two fluids are calibrated, the hot and cold circuits of the exchanger are reconstructed, and the overall pressure drops are estimated. Moreover, the

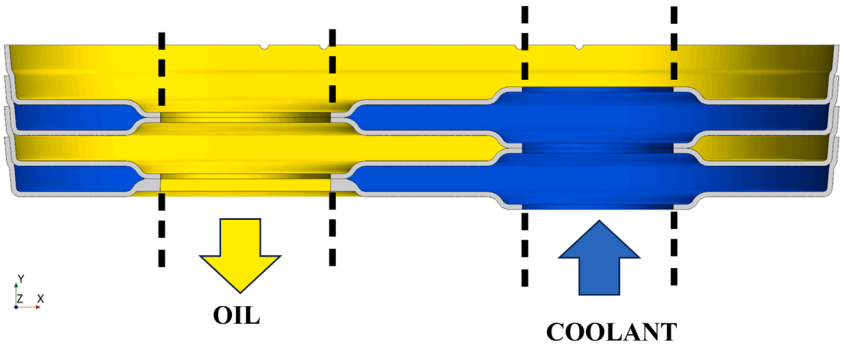

Fig. 1. Scheme representing oil and water hydraulic circuits.

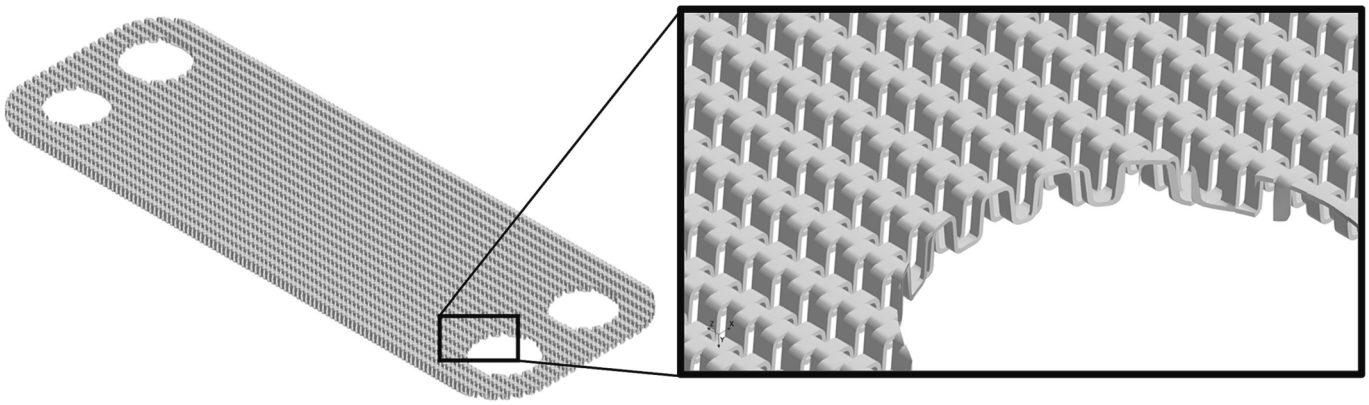

Fig. 2. Turbulators geometry.

reduced two-plate exchanger allows the estimation of the overall heat transfer between the fluids. A REV is only adopted to perform a sensitivity to both mesh and turbulence models quickly. Even if the proposed methodology involves different numerical frameworks (some of them requiring a non-negligible computational effort), it is much easier than the existing ones based on REVs. In fact, as in the present paper, it can be applied by means of commercial codes and it does not require user-coding. Moreover, it remains still quicker and much more affordable than the simulation of entire devices.

In order to validate the robustness of the methodology, CFD results are compared to experimental data of heat transfer and pressure drop on an oil/water cooler.

The resulting method is robust in terms of accuracy, thanks to the satisfying agreement with respect to the experimental evidence. Moreover, it is affordable in terms of the required computational effort.

The paper is organized as follows. Firstly, the investigated exchanger is presented and described along with the experimental data. Then, the proposed methodology and the numerical setup are described. The following section proposes sensitivities to both mesh and turbulence model carried out on the REV. The last section discusses the results in terms of heat transfer obtained on the periodic two-plate model and the outcomes of pressure drop provided by the porous media. Finally, conclusions are drawn.

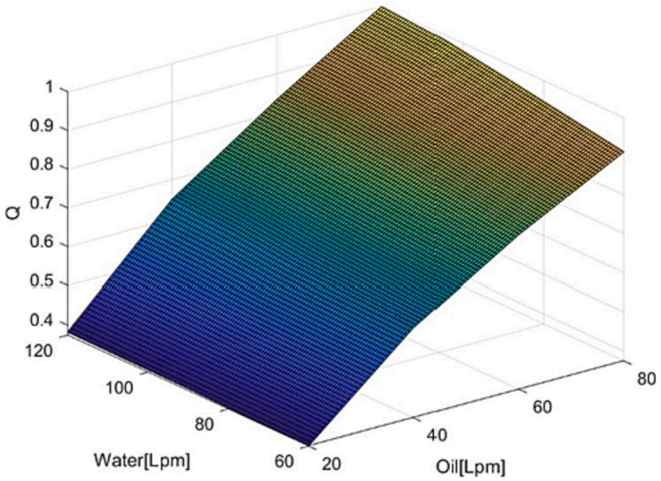

Fig. 3. Normalized heat transfer.

2. Investigated heat exchanger and experimental data

The investigated device is a brazed plate-fin heat exchanger adopted in high specific power engines as an oil cooler. A sketch of the section is reported in Fig. 1, which shows how each fluid fills the plates

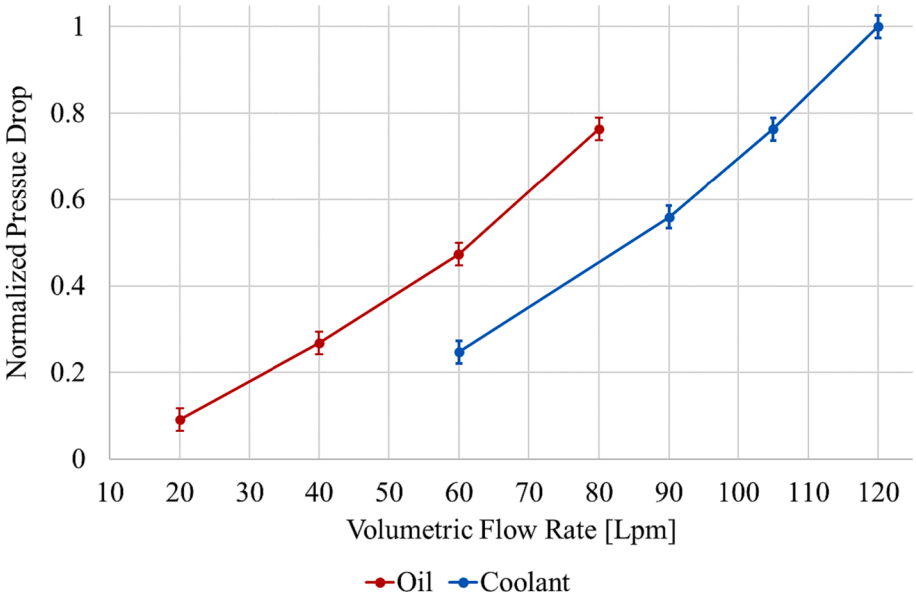

Fig. 4. Normalized pressure drop.

alternatively.

As it can be noticed in the section, turbulators are present inside each plate. The texture of the turbulators is shown in Fig. 2, along with a detail of the geometry, which is characterized, de facto, by staggered arrays of wavy fins, aiming at enhancing turbulence and, thus, convective heat transfer.

As for the experiments, data are available in terms of heat transfer and pressure drop. In particular, thanks to temperature measurements at inlet and outlet, the heat rejected to the coolant (water) by the oil is estimated. Temperature measures involve both the fluids (despite just one would be enough to estimate the heat transfer between them), thus providing a double check of the quality of the data. The pressure drop is obtained via pressure sensors at inlet and outlet and, once again, measures involve both water and oil as the losses are strongly different for the two fluids. Experimental data are resumed in Figs. 3 and 4, where values of exchanged thermal power and pressure drop are reported in a dimensionless form for the sake of confidentiality. The maximum values measured at the bench are used to make the measures dimensionless. As for the test facilities, the test rig exploits a chiller and two separate heaters to keep the fluid temperatures at the working conditions. The heat exchanger is wrapped in glass wool batt to minimize the heat transfer with the external environment. Four resistive temperature sensors (Pt1000) and two piezoresistive pressure sensors are positioned at each inlet and outlet to measure the outlet temperatures and pressures and double-check the inlet conditions of the fluids. Temperature and pressure sensors are characterized by an accuracy of $\pm 0.5\ ^{\circ}C$ and $\pm 0.2\%$ of the full scale, respectively. Finally, two Coriolis-effect flowmeters monitor the supplied mass flows, with an accuracy of $\pm 0.2\%$. The resulting uncertainties for the pressure drop and heat transfer measurements are added to the graphs by means of error bars.

3. Numerical set-up

The 3D-CFD simulations are carried out with STAR-CCM + v17.02, licensed by SIEMENS DISW. Turbulence is treated with a RANS (Reynolds Average Navier-Stokes) approach. Time-dependency is neglected (i.e. steady-state simulations are considered) thus all the time-dependent terms are omitted in the conservation equations reported in the following and adopted by the solver. Eqs. (1), 2 and 3 express the conservation of mass, momentum and energy, respectively.

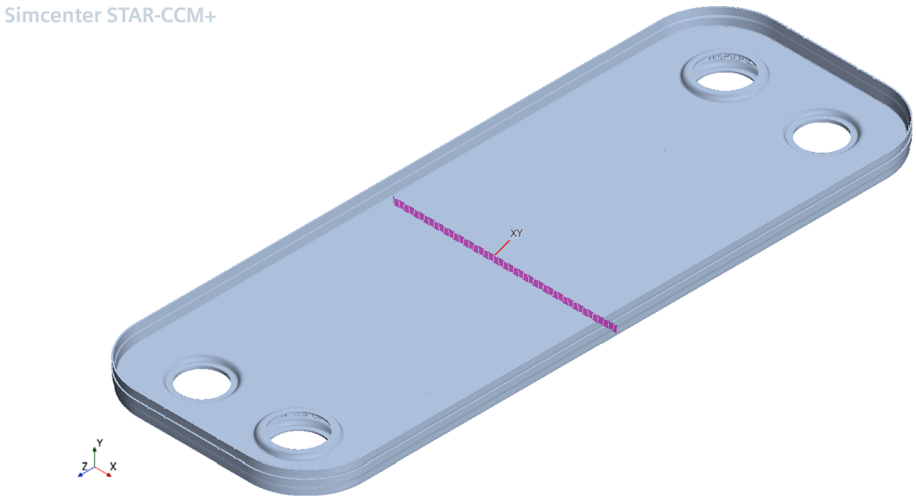

Fig. 5. Mid-section of the plate.

$$\frac{\partial \overline{\rho}}{\partial t}+\frac{\partial(\overline{\rho}\widetilde{u_i})}{\partial x_i}=0 \tag{1}$$

$$\frac{\partial(\overline{\rho}\widetilde{u_i})}{\partial t}+\frac{\partial}{\partial x_j}\left(\overline{\rho}\widetilde{u_i}\widetilde{u_j}+\rho\overline{u_i''u_j''}\right)=-\frac{\partial(\overline{\rho}\delta_{ij})}{\partial x_j}+\frac{\partial\overline{\tau_{ij}}}{\partial x_j} \tag{2}$$

$$\frac{\partial(\overline{\rho}\widetilde{e_o})}{\partial t}+\frac{\partial}{\partial x_j}\left(\overline{\rho}\widetilde{u_i}\widetilde{e_o}+\rho\overline{u_j''e_o''}\right)=-\frac{\partial\widetilde{u_j}\overline{p}}{\partial x_j}-\frac{\partial\overline{u_j''p}}{\partial x_j}+\frac{\partial\overline{u_i\tau_{ij}}}{x_j}-\frac{\partial\overline{q_j}}{\partial x_j} \tag{3}$$

density, "ρ ", is considered as a variable term; therefore, both Favre and Reynolds averaging techniques are adopted. The ensemble average operator is indicated as "-", while the density-weighted average operator is expressed via "~". Velocity components, shear stresses, pressure, energy, specific heat transfer and Kronecker delta are referred to as $u_{i,j}$, $\tau_{i,j}$, p, e_o, q and δ_{ij}, respectively.

Assuming an equal distribution of the mass flow rate among the plates, the average Re numbers at the mid-section of each plate highlighted in Fig. 5 range (based on the operating condition) between 2000 and 4500 for water and between 50 and 200 for oil. However, such values represent an approximation of the actual Re number, as the mass flow rate is not equally distributed among the plates, neither it is uniform in the section.

Although the Re numbers (mostly the oil one) do not suggest the presence of turbulent phenomena, the adoption of a turbulence model in the proposed simulations is necessary because of two different reasons. The first one is the size of the hydraulic diameter, which is equal to D_h = 1.8 mm, calculated as $D_h = 4*V/A_s$, where A_s is the wet surface area and V is the volume of the fluid. Several authors pointed out that the geometric characteristics of the channels, such as the aspect ratio [30] and the size of the hydraulic diameter affect the threshold of the Re number for the laminar-to-turbulent transition. Kandlikar *et al.* [31] classified channels with a hydraulic diameter below 3 mm as mini-channels and pointed out that the critical Reynolds number of such channels is reduced with respect to the ones characterized by larger hydraulic diameter.

The second one is the presence of turbulators which promote separation phenomena enhancing the onset of a turbulent flow.

Different turbulence models are tested in the present study. Among them, the Reynolds-Stress-Transport (RST) model is preferred since it is the most suitable (as indicated by the results that will be shown later on) to face the thermo-fluid dynamic analysis of the exchanger under investigation. For this reason, the main features of the RST model are briefly resumed in the following. In particular, the details of the adopted specific version are presented.

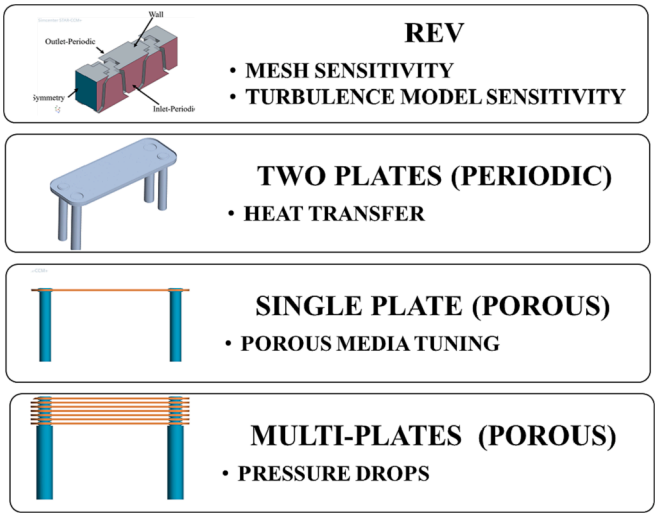

Fig. 6. Summary of the adopted numerical methodology.

The RST model directly calculates the components of the Reynolds stress tensor by solving dedicated transport equations that are resumed in Eq. (4), following the nomenclature adopted in the code manual [32].

$$\frac{\partial(\rho\mathbf{R})}{\partial t}+\nabla(\rho\mathbf{R})=\nabla\bullet\mathbf{D}+\mathbf{P}+\mathbf{G}-\frac{2}{3}\mathbf{I}\gamma_M+\underline{\phi}-\rho\underline{\varepsilon}+S_R \tag{4}$$

$\boldsymbol{P}$ is the turbulent production term, $\boldsymbol{D}$ is the Reynolds stress diffusion term, $\boldsymbol{G}$ is the Buoyancy production term, $\boldsymbol{I}$ is the identity tensor, $\underline{\varepsilon}$ is the turbulent dissipation rate tensor, γ_M is the dilatation dissipation (which is modeled as in the $k-\varepsilon$ model), S_R is the user specified source and, finally, $\boldsymbol{R}$ is the Reynolds stress tensor which is reported in Eq. (5).

$$\boldsymbol{R}=\begin{bmatrix}\overline{u'u'} & \overline{u'v'} & \overline{u'w'}\\ \overline{v'u'} & \overline{v'v'} & \overline{v'w'}\\ \overline{w'u'} & \overline{w'v'} & \overline{w'w'}\end{bmatrix} \tag{5}$$

The RST has the potential to predict complex flows more accurately than Eddy Viscosity models, as the RST equations naturally account for the effect of turbulence anisotropy, curvature of the streamlines and swirl motion.

The RST is characterized by the presence of different versions, based on the modeling of the pressure-strain tensor ($\underline{\phi}$**).** In particular, the specific version selected for the simulations of the exchanger is the Linear Pressure Strain (LPS), proposed by Launder *et al.* [33,34,35,36] where the pressure strain tensor is described by five different components, as visible in Eq. (6).

$$\underline{\Phi}=\underline{\Phi}_s+\underline{\Phi}_r+\underline{\Phi}_{r,b}+\underline{\Phi}_{1w}+\underline{\Phi}_{2w} \tag{6}$$

As described by Wilcox *et al.* [37], the rapid pressure-strain term $\underline{\phi_r}$ is responsible for capturing the effects of small-scale turbulence structures on the Reynolds stress. The slow term $\underline{\phi_s}$ depends on the deformation of the mean velocity field and is resposible for capturing the effects of large-scale turbulence structures. Finally, $\underline{\phi_{r,b}}$ represents the buoyancy contribution term. $\underline{\phi_{1w}}$ and $\underline{\phi_{2w}}$ are the rapid and slow wall-reflection terms, which take into account the effect of the proximity to a solid boundary on the rapid and slow pressure strain terms, respectively [35,36].

In order to describe the near-wall flow, the so called 'two-layer' approach proposed by W. Rodi [38] is adopted. The computation is divided in two layers: near the wall, the turbulent dissipation rate ε and the turbulent viscosity μ_t are specified as a function of the wall distance, according to the Wolfstein formulation [39,32]. Far from the wall, ε and μ_t are calculated as in the RST model, that is the turbulent dissipation rate is computed by the transport equation while the turbulent viscosity is calculated as in $k-\varepsilon$ models. A blending procedure is then adopted to smooth the transition between the two layers. For example, μ_t is calculated as in Eq. (7), where λ is a wall-proximity indicator defined by Eq. (8) as suggested by Jongen [40], μ is the dynamic viscosity, $\left(\frac{\mu_t}{\mu}\right)_{Wolfstein}$ is the (dimensionless) turbulent viscosity for near-wall layer provided by the Wolfstein formulation and $\mu_{t_{RST}}$ is the turbulent viscosity expression away from the wall. The width of the wall proximity indicator, A, is determined via Eq. (9), where Re_d is the wall distance Reynolds number reported in Eq. (10). In these equations, k is the turbulent kinetic energy, d is the wall-distance and ν is the kinematic viscosity. Moreover, ΔRe_y and Re_y^* are model coefficients fixed to 10 and 60, respectively.

$$\mu_t=\lambda\mu_{t_{RST}}+(1-\lambda)\mu\left(\frac{\mu_t}{\mu}\right)_{Wolfstein} \tag{7}$$

$$\lambda=\frac{1}{2}\left[1+\tanh\left(\frac{Re_d-Re_y^*}{A}\right)\right] \tag{8}$$

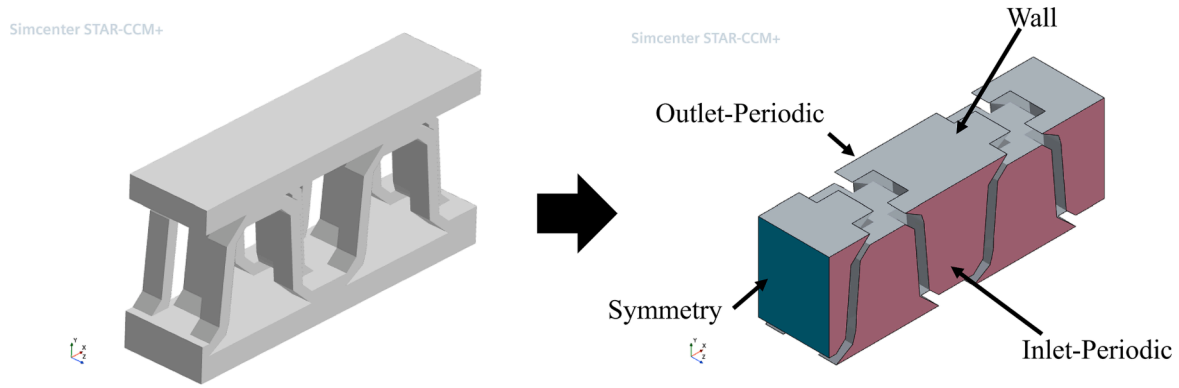

Fig. 7. Representative elementary volume.

$$A = \frac{|\Delta Re_y|}{\text{atanh}(0.98)} \tag{9}$$

$$Re_d = \frac{(\sqrt{k}\, d)}{\nu} \tag{10}$$

The two-layer version of the RST model enables integration of the governing equations up to the wall, i.e. the near-wall cell centroid can fall inside the viscous sub-layer. However, also the case of centroids pertaining to the log-region is properly supported. For this reason, as for the near-wall treatment, an all-y^+ approach is adopted, which provides correct boundary conditions for flow, energy and turbulence regardless of the y^+ value. For example, the wall shear stress (provided by the wall treatment) depends on the dimensionless velocity (u^+) which is formulated blending the linear profile (exact boundary condition) and the log one (velocity wall function), in order to adapt to the y^+ value. Further details can be found in [32].

4. The proposed methodology

The proposed methodology relies on four different numerical frameworks, as schematically reported in Fig. 6. The first framework focuses on a small element representative of the geometry and it is dedicated to mesh and turbulence model sensitivities. The second one extends the domain to a subsystem of the heat exchanger (two plates) and it provides estimations of heat transfer and pressure drops. As for the heat transfer, it is a portion of the overall amount associated to the exchanger (in fact the total heat transfer can be easily calculated multiplying the value from the simulation by the number of plate pairs of the device). The data concerning the pressure drops of the two fluids are exploited in a further framework based on a single porous plate which is alternatively exploited for both the fluids in order to calibrate the respective porous media. Finally, these last are adopted in the fourth framework to simulate the entire hydraulic circuits associated to each fluid inside the exchanger. The goal is the estimation of the overall pressure drops.

A more detailed description of each framework is proposed in the following paragraphs.

4.1. The representative elementary volume (REV)

The first framework is reported in Fig. 7 and focuses on an extremely restricted computational domain, but still representative of the geometry of a single plate (which is periodic in the core, as characterized by regular patterns of turbulator arrays). The REV is exploited to minimize the domain extension [25] thus reducing the computational time required to carry out sensitivity analyses to mesh size and turbulence models, as proposed in [41]. In order to eliminate the effect of the boundary conditions and obtain a solution representative of a fully developed flow (which should mimic the repetitive fluid dynamics inside the plate), the inlet and the outlet boundaries are linked by means of a periodic condition. The other boundaries are set as symmetry planes (to account for the presence of the fluid) or walls (in correspondence of turbulators and plates). The interface associated to the two periodic boundaries allows to obtain a fully developed flow, as well as to specify a mass flow rate.

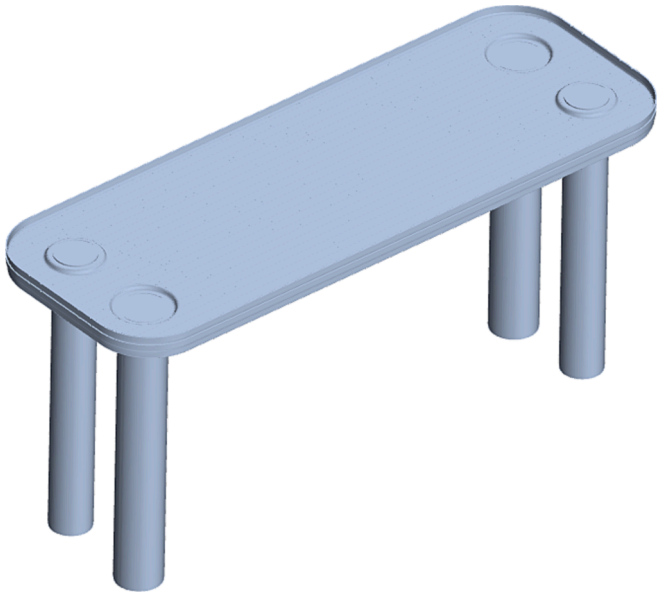

Fig. 8. Periodic two plate exchanger geometry.

4.2. The periodic two plate exchanger

As stated earlier, the presence of an articulated geometry inside the plates makes the 3D-CFD analysis of the entire device unfeasible for the computational resources commonly available in both industrial and research fields. Quantitatively, as a result of the mesh sensitivity analysis which will be presented afterwards, the mesh of the complete geometry is estimated to be made up of nearly 800 million cells. The workstation adopted by the authors, characterized by 32 cores and 130 Gb of RAM is not able to even execute such a mesh.

As a solution, the simulation domain is reduced to only two plates, one associated to the oil and one to the water, required to model the heat exchange process, as visible in Fig. 8.

Periodic boundaries are then imposed to mimic the presence of the adjacent plates, which exchange heat with the two simulated ones. In fact, as for the simulated water plate, the lower boundary should be in

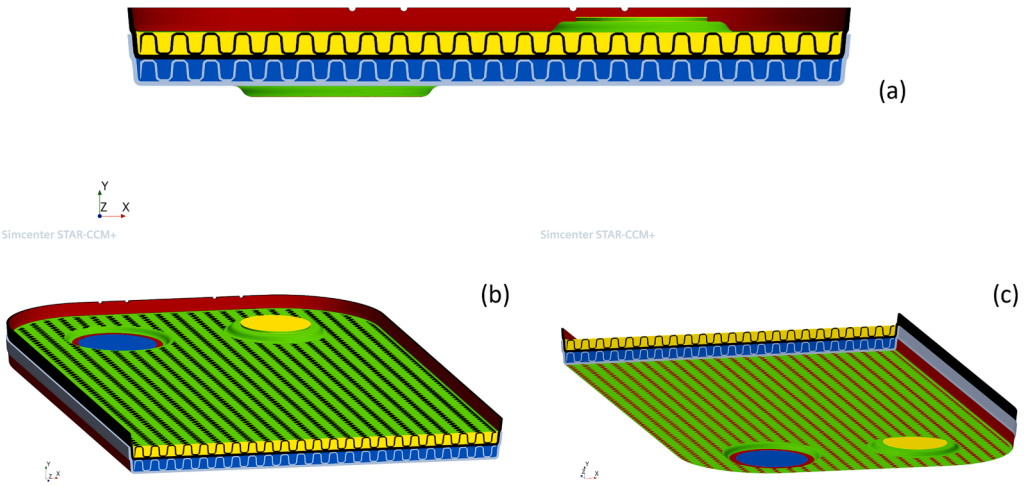

Fig. 9. Section of the periodic two-plate exchanger. Oil and water volumes are depicted in yellow and blue respectively. Lower plate and turbulators are grey colored, while the upper ones are black. Periodic contacts between the solids are red. Periodic contacts between oil and lower plate are green.

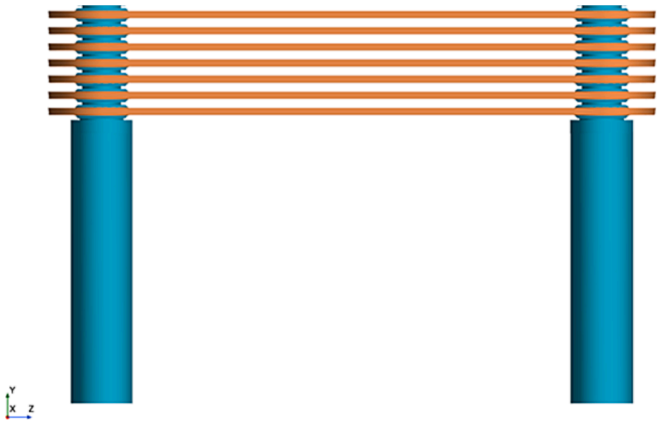

Fig. 10. Geometry of a single fluid circuit. Two different region types can be distinguished: the blue one (fluid) describing the channels associated to inlets/outlets and the orange one (porous) associated to the plates.

contact with an oil plate roughly at the same conditions (of flow and thermal field) as the simulated one. The same applies for the upper boundary of the simulated oil plate. Fig. 9 shows the considered domain and the periodic contacts are highlighted.

The estimation of the total heat rejected in the exchanger from the hot fluid to the coolant is obtained by multiplying the heat rejection associated to the two simulated plates by the number of plate couples. It is important to point out that this approach assumes the mass flow rate to be equally distributed among the plates, and the number of plates to be sufficiently high to neglect that the extremal plates exchange heat only on one side. Unfortunately, the flow is highly tridimensional within the exchanger, i.e. the mass flow rate is not equally distributed between the plates (and not even uniform inside each one). However, since the heat transfer is roughly linear with the mass flow rate (i.e. with the velocity), it is still possible to investigate only a couple of plates characterized by an average mass flow rate, computed as the total mass flow rate divided by the number of plates.

4.3. The porous water and oil circuits

In the estimation of the pressure drop across the exchanger there is a main critical issue: the simulation of the entire device is not feasible even considering a single fluid at a time, i.e. two separated circuits as in Fig. 10.

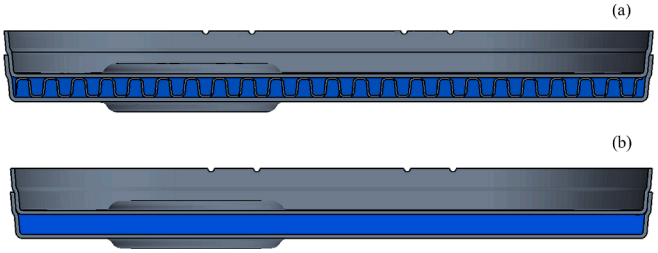

Fig. 11. Comparison, for a single plate, between the actual geometry (a) and the porous version (b).

Therefore, it is necessary to recover the solution widely adopted in literature and based on the adoption of a porous medium, which enables the simulation of complex periodic geometries with a limited computational cost. The circuit of each fluid inside the device is simplified, i.e., the turbulators are eliminated. Consequently, the number of cells required to discretize each plate is strongly reduced and the fluid volume is now described as a porous medium. Fig. 11 shows the difference between an original plate (any one of the heat exchanger) and the corresponding version made of porous medium.

The pressure drop associated to a porous medium has to be tuned by the porous model parameters to match a desired target. The adopted code models the pressure loss in the porous region by introducing a sink in the momentum equation, which is given by the volume integral of the porous medium resistance force $\mathbf{f_b}$, whose expression is reported in Eq. (11).

$$\mathbf{f_b} = -\mathrm{P} \bullet \mathbf{v_s} \tag{11}$$

$\mathbf{v_s}$ is the superficial velocity, which is related to the physical velocity ($\mathbf{v}$) by means of the porosity (χ) of the porous medium as in Eq. (12).

$$\mathbf{v_s} = \chi \bullet \mathbf{v} \tag{12}$$

The porosity χ of the porous medium is calculated in Eq. (13) as the ratio between the volume occupied by the fluid (V_f) and the total volume of a cell (V).

$$\chi = \frac{V_f}{V} \tag{13}$$

$\mathbf{P}$ is the porous resistance tensor and it is obtained as in Eq. (14).

$$\mathbf{P} = \mathbf{P_v} + \mathbf{P_i}|\mathbf{v_s}| \tag{14}$$

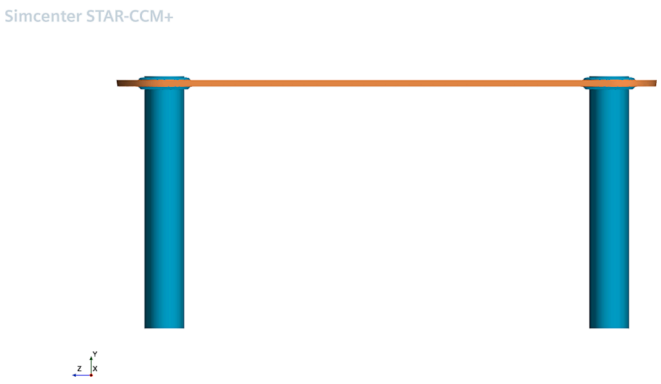

Fig. 12. Single plate geometry.

$\mathbf{P_i}$ and $\mathbf{P_v}$ are the inertial and viscous resistance tensors, respectively. In the present activity, both tensors are considered isotropic. Therefore, they reduce to two coefficients that can be tuned to match the required pressure drop. For simplicity, only $\mathbf{P_i}$ is tuned while $\mathbf{P_v}$ is fixed to 0. The reason is that the porous medium is ad hoc calibrated for each operating condition, thus only one coefficient is sufficient to match the single pressure drop. $\mathbf{P_v}$ can be used instead of $\mathbf{P_i}$ with the same final result. The adoption of both coefficients to compose the tensor **P (**as it is usually done in practice) would lead to infinite combinations providing the same result and is therefore discarded.

It is important to point out that the calibration of the porous medium is necessary for each condition for two reasons. The first one is that $\mathbf{P_i}$ and $\mathbf{P_v}$ are considered, for simplicity, isotropic even if they are not. The calibration of $\mathbf{P_i}$ and $\mathbf{P_v}$ on two conditions (solving a system of two equations and two unknowns) and their use at further points would lead to a non-negligible error in the prediction of the pressure drop. On the contrary, a case-by-case calibration forces to match the pressure drop even if the tensors are erroneously approximated as isotropic.

The second one is that it is not possible to ignore the heat transfer effect and the related variation of temperature-dependent physical properties of the two involved fluids. Since all the pressure drop measurements are carried out during the device operation, thus in presence of heat transfer, the temperature of the fluids changes, leading to variation of their physical properties, such as the dynamic viscosity. The latter does not sensibly vary for the water in the range of temperature experienced by the fluid during the operation, but the same is not valid for the oil. The variation of the viscosity for the latter has a strong impact on the pressure drop. The point is that the effect of the heat transfer varies with the operating point. In fact, based on the operating condition, the temperature difference of the fluids between inlet and outlet varies and, thus, the properties modify as well. For this reason, the calibration of the porous medium has to be carried out on a point-by-point basis.

In order to tune the porous medium for each fluid and for each operating point, a single plate is considered, as the one in Fig. 12. Similarly to Fig. 10, the blue region is fluid, while the orange one is porous. As discussed above, the plate (orange region) is empty as the turbulators are now modeled via a porous medium. In order to consider the effect of the thermal gradient on the pressure drop, Stogiannis *et al.* [42] imposed an a-priori-defined linear thermal gradient on the wall boundaries of the simulated plate. Instead, in the present approach, the pressure drop is calibrated to match the pressure drop resulting from the simulation on the two-plate exchanger presented in the previous paragraph. This allows not only to account for the effect of the turbulators, but also for the effect of the heat transfer similarly to a plate of the original multi-plate exchanger.

Once the porous medium parameters are calibrated, the porous version of the multi-plate geometry reported in Fig. 10 is exploited, for both the fluids, to calculate the pressure drop along the whole circuits.

Interestingly, the porous media (single plate and multi-plate) of the two fluid circuits are isothermal, in fact the heat transfer effect is already accounted for in the calibration of the porous medium constants. This allows to keep the porous-medium-based models as simple as possible.

Given the above, the proposed methodology for the estimation of the pressure drop can be resumed as follows:

1. The pressure drop is evaluated for each fluid by the two-plate model (thus the effect of the heat transfer is included).
2. The porous-medium-based single plate model is initially tuned (acting on $\mathbf{P_i}$) for water, at isothermal condition, to obtain the pressure drop calculated at point 1 by the actual geometry (two plate model) on the water side. Then, the same porous-medium-based single plate model is tuned for oil (simply changing the fluid properties), to reproduce the pressure drop obtained at point 1 by the actual geometry (two plate model) on the oil side.
3. Finally, the isothermal multi-plate porous-medium-based model is adopted. It is run twice, one for water and one for oil, with the respective $\mathbf{P_i}$ values calculated at point 2. It estimates the overall pressure drops caused by the exchanger on the two fluids. Interestingly, the isothermal multi-plate porous-medium-based model may not be the same for the two fluids. In fact, if the total number of plates is odd, the number of plates pertaining to each fluid is different.

Before moving to the results, it is important to point out that the adoption of porous media has the only goal to estimate the total pressure drop. No information about the flow inside each plate can be inferred because of the isotropic approximation of the porous media. In this regard, the analysis of the flow field inside the plates can be carried out by the two-plate model.

5. Results

5.1. Mesh sensitivity

The mesh sensitivity analysis is performed separately for the two fluids (namely oil and water) because of their different properties and volumetric flow rates and also because the REV can account for only one fluid at a time. The mass flow rate specified at the interface is set ad-hoc for each fluid in order to replicate the flow condition experienced by the actual heat exchanger. In particular, the adopted values aim at reproducing the condition of maximum flow rate. This roughly corresponds, de facto, to the adoption of a mass flow rate given by the one that flows through a plate at the condition of maximum flow rate of the exchanger, multiplied by the ratio between the section of the REV and the total section of the plate.

A polyhedral mesh and a prism layer mesh are adopted in the bulk region and near the wall, respectively. The adopted mesh sensitivity workflow is the following. Firstly, the dimension of the mesh in the bulk region is investigated for a given prism layer near the wall. In particular, the bulk mesh is refined until the pressure drop across the REV does not change anymore. Then, different prism layer meshes are tested to achieve a grid-independent estimation of the pressure loss. Both for the bulk and the near-wall region, the selected mesh is the one that minimizes the computational cost, while ensuring reasonably grid-independent results.

For the selected dimension of the bulk, the prism layer mesh is investigated by varying the number of layers and adjusting the growth rate to maintain a smooth transition to the bulk region, on equal height of the first layer. The height of the first layer is chosen equal to 30 μm, which allows to keep the value of y^+ below 5. In fact, despite the all-y^+ wall treatment allows both a high-Reynolds and a low-Reynolds approach (the switch between the two only depends on the local y^+ value), the dimensionless distance value is kept low enough to enable a low-Reynolds wall treatment, to improve the estimation of the wall quantities. Four different prism layer configurations are tested with increasing number of layers (up to ten).

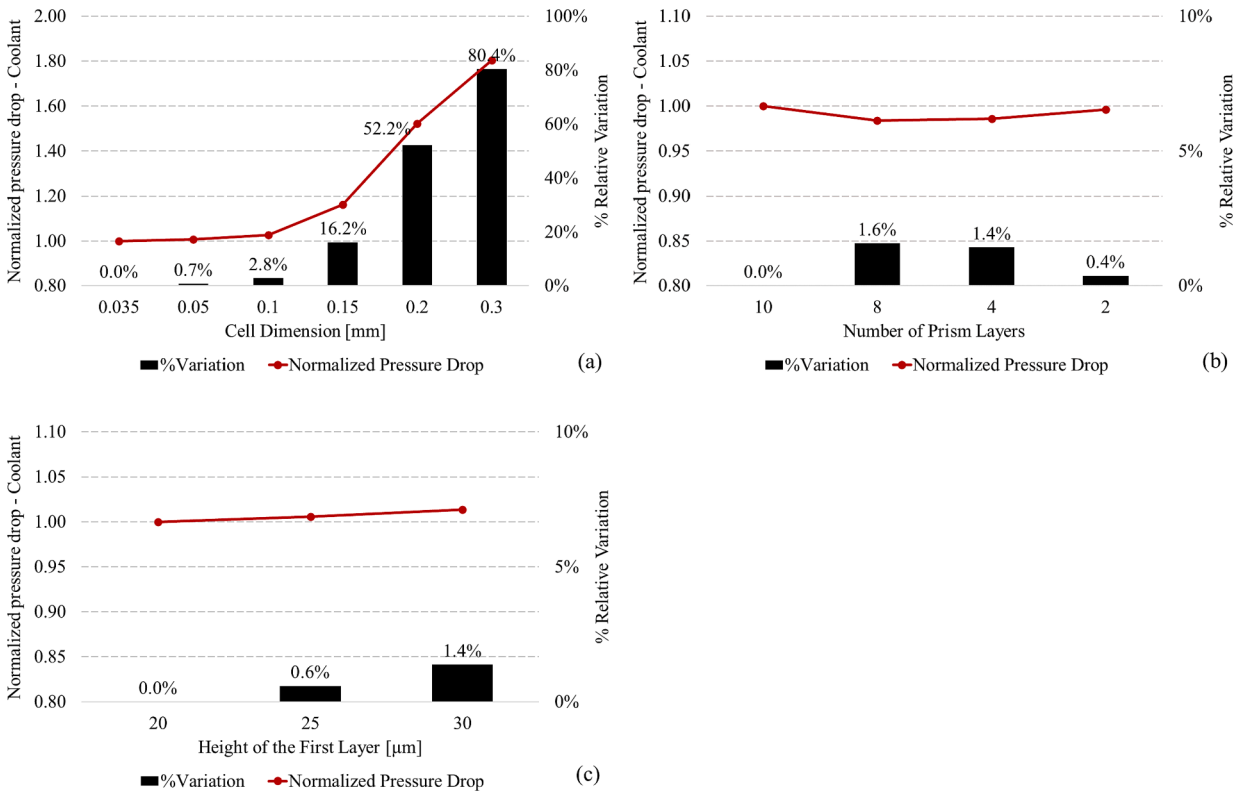

Fig. 13. Mesh sensitivity analysis on the REV for water. a) Sensitivity to the bulk cell dimension; b) sensitivity to the number of prism layers; c) sensitivity to the height of the first layer.

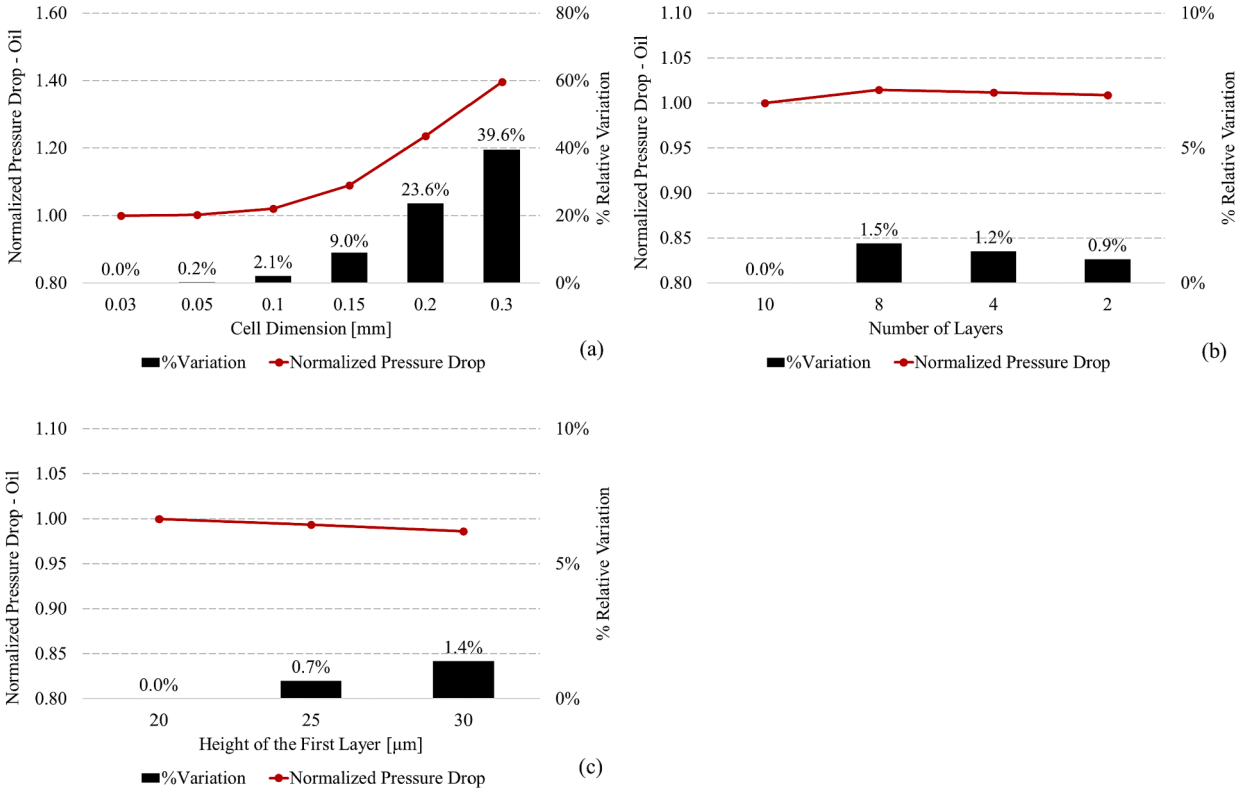

Fig. 14. Mesh sensitivity analysis on the REV for oil. a) Sensitivity to the bulk cell dimension; b) sensitivity to the number of prism layers; c) sensitivity to the height of the first layer.

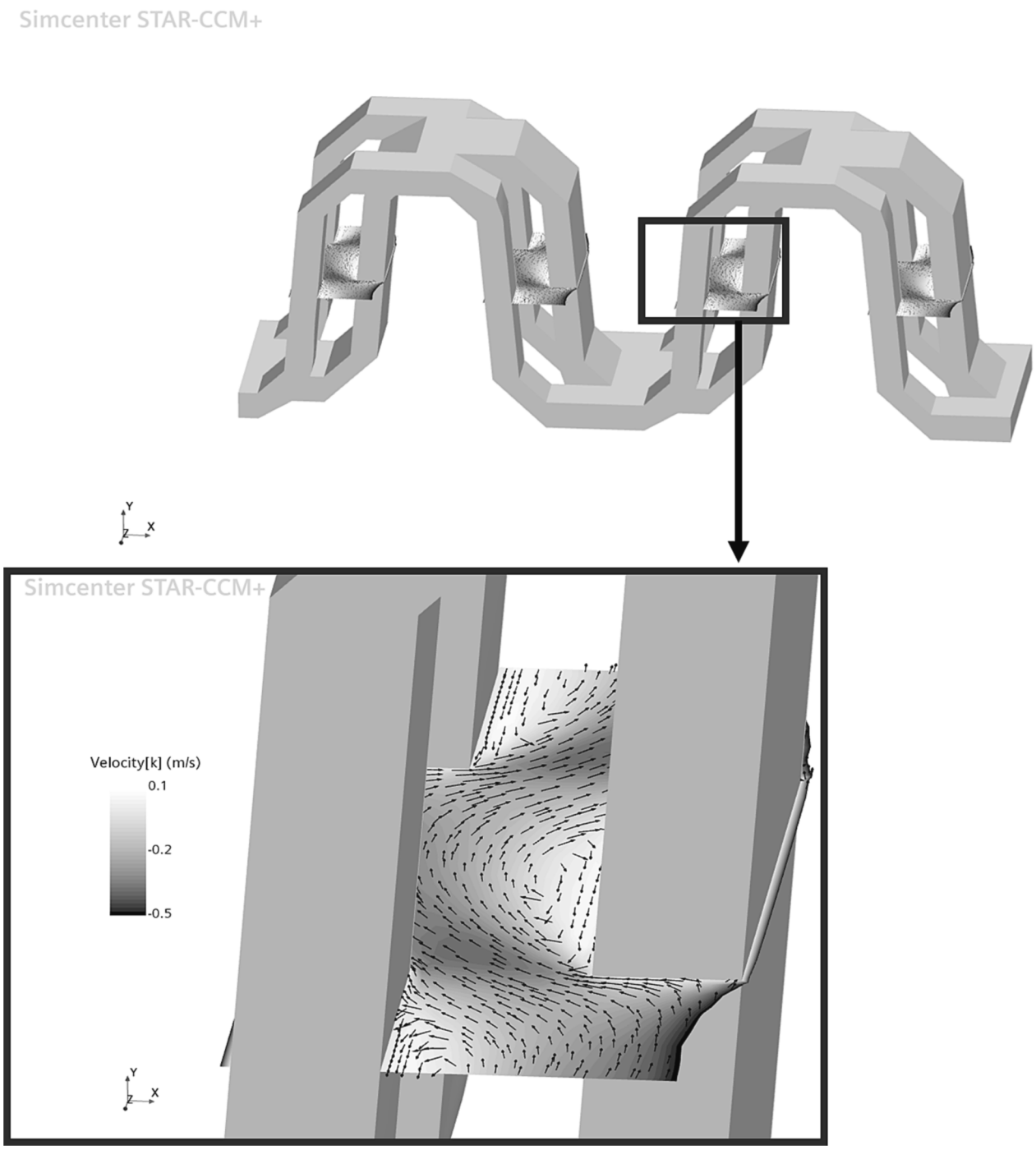

Fig. 15. Field of the k-component (that is along z-direction) of the velocity is shown along with velocity vectors. A close-up to highlight the presence of a recirculation zone is proposed. The direction of the flow is towards negative z. The simulation is performed with a mesh having a constant size for the cell of the bulk region of 0.05 mm and a prism layer composed of two layers only.

Finally, different heights of the first layer are considered, all of them enabling a low-Reynolds wall treatment as the y^+ keeps sufficiently low. It is useful to point out that, for the mesh sensitivity analyses, the turbulence effect is accounted for via the RST-LPS model described in the previous paragraph.

Starting from water, the analysis shows that a grid-independent solution is achieved for a dimension of the bulk mesh of 0.05 mm, as visible in Fig. 13a). In fact (almost) halving the size leads to a variation of the pressure drop lower than 1 %. It is worth to point out that such a mesh requires almost half a million cells, even though the volume considered is just a small portion of the overall geometry. This forces the adoption of a coarser mesh with a characteristic bulk size of 0.15 mm, thus accepting a relative variation of nearly 10 % with respect to the grid-independent value obtained with the size equal to 0.05 mm. The resulting reduction of cells is nearly of 16 times. The small variation of the pressure drop associated to a modification of the number of layers (Fig. 13b)) allows to limit their number to two. The tests on the first layer show an acceptable variation of the results altering the height (Fig. 13c)). Therefore, a height of 30 μm (the greatest value) is selected.

The mesh sensitivity analysis for the oil is carried out in the same way and results are reported in Fig. 14a), b) and c). Similarly, to water, a grid-independency is achieved with a dimension of the bulk mesh of

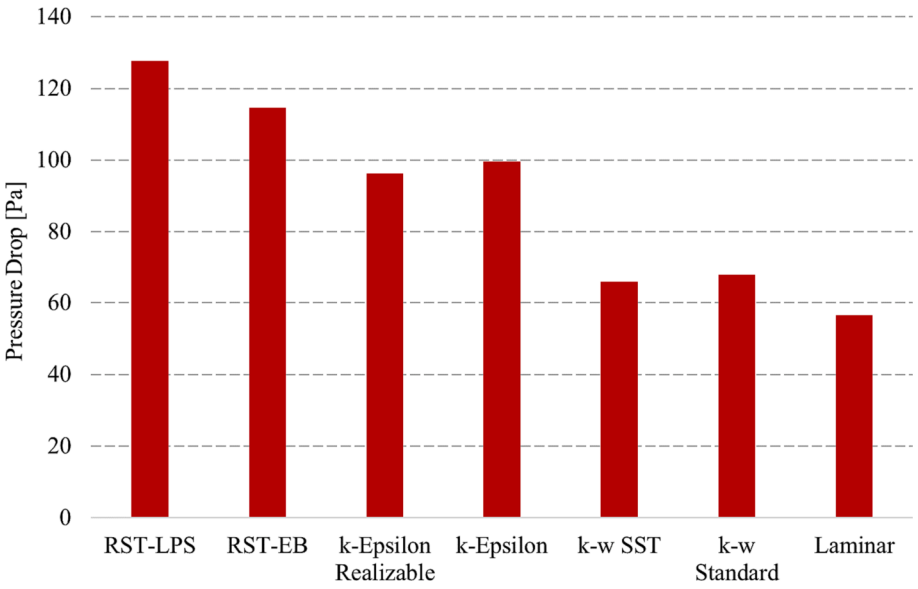

Fig. 16. Pressure drop registered over the REV for different turbulence models.

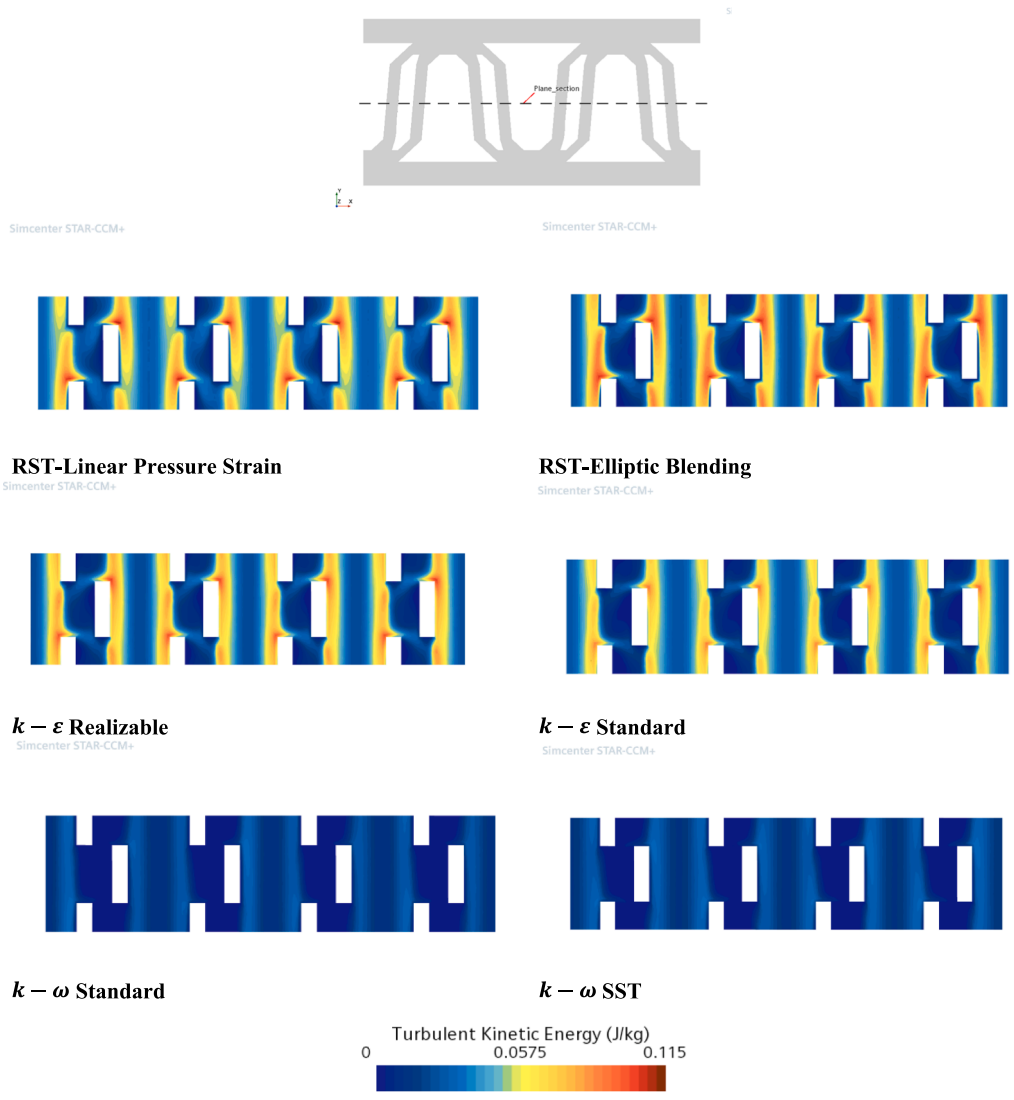

Fig. 17. Turbulent kinetic energy over a section of the REV.

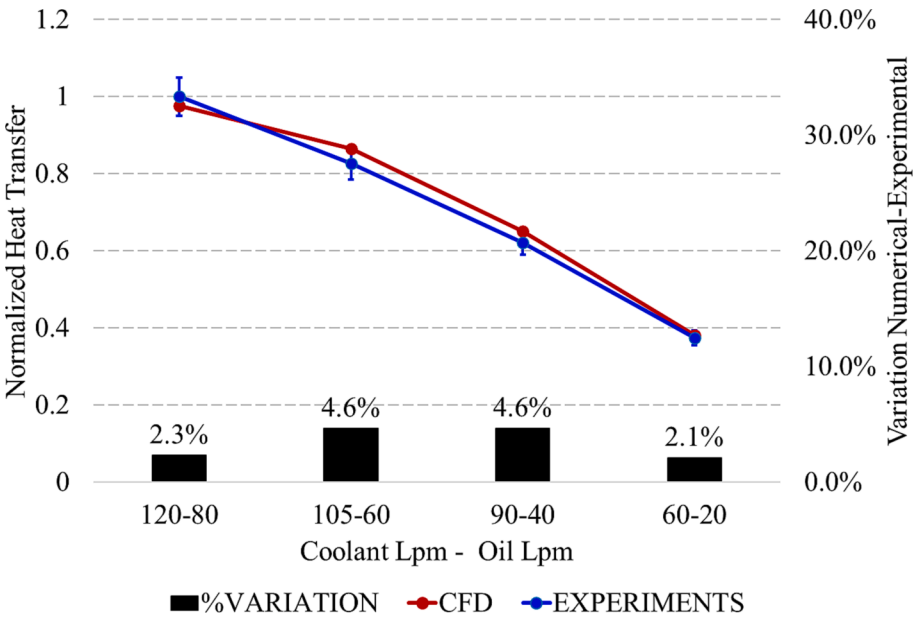

Fig. 18. Comparison between simulations and experiments in terms of normalized heat transfer.

0.05 mm. Even in this case, a size of 0.15 mm is preferred along with two layers at the walls and the first of 30 μm. For this fluid, the accepted error (i.e. variation with respect to the bulk grid-independent value) is 9 %.

5.2. *Turbulence model sensitivity*

As anticipated in the numerical setup paragraph, even the modeling of the oil side requires a turbulence model, despite the Reynolds number related to the highest volumetric flow rate is lower than 500. Indeed, even if not reported for brevity in the paper, preliminary simulations are run with a laminar approach and show a non-negligible underprediction of the pressure drop compared to the experiments. In order to explain such a behavior, in Fig. 15 the results on the REV obtained in the previous paragraph for the oil are presented. As visible, the presence of recirculation zone behind the turbulators leads to the presence of localized turbulent phenomena which require an ad-hoc modeling by adopting a turbulence model. As for the water side, on equal geometry, the higher Reynolds numbers due to both the lower viscosity and the higher volumetric flow rates make the adoption of a turbulence model even more necessary.

Different turbulence models are tested to obtain a proper estimation of the pressure drop across the exchanger. The choice of the turbulence model is driven by an iterative process. The first trials exploit the well-diffused $k-\varepsilon$ and $k-\omega$ models and result in a strong underprediction of the pressure losses when compared to the experiments. Therefore, the Reynolds stress tensor models are tested. The RST Linear Pressure Strain model is selected as the one giving the best match with experimental results. In order to speed up the research of the optimal numerical setup, a sensitivity analysis of the pressure drop to the turbulence model on the REV is considered. Different turbulence models available in the code are tested, namely:

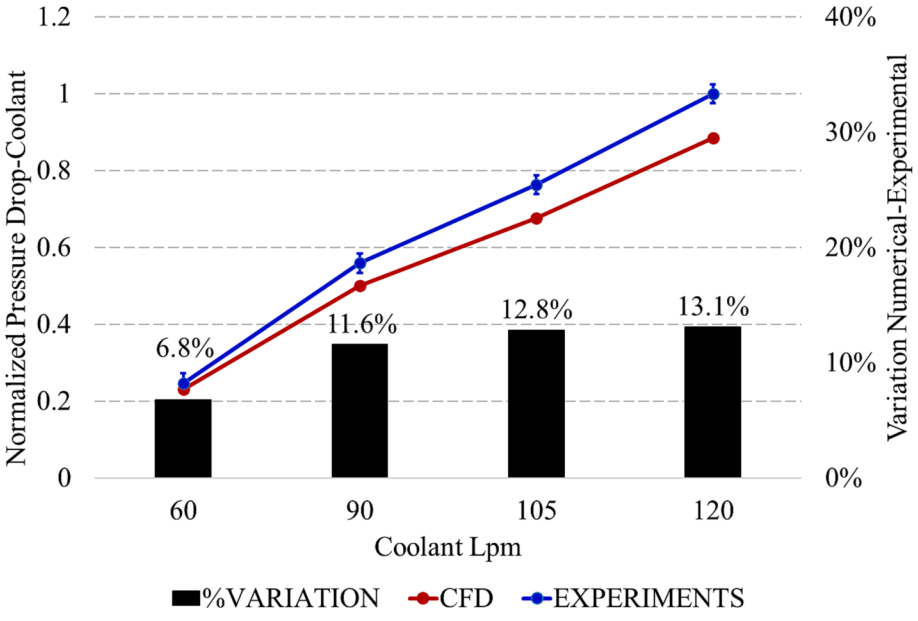

Fig. 19. Comparison between simulations and experiments in terms of normalized pressure drop of the water circuit.

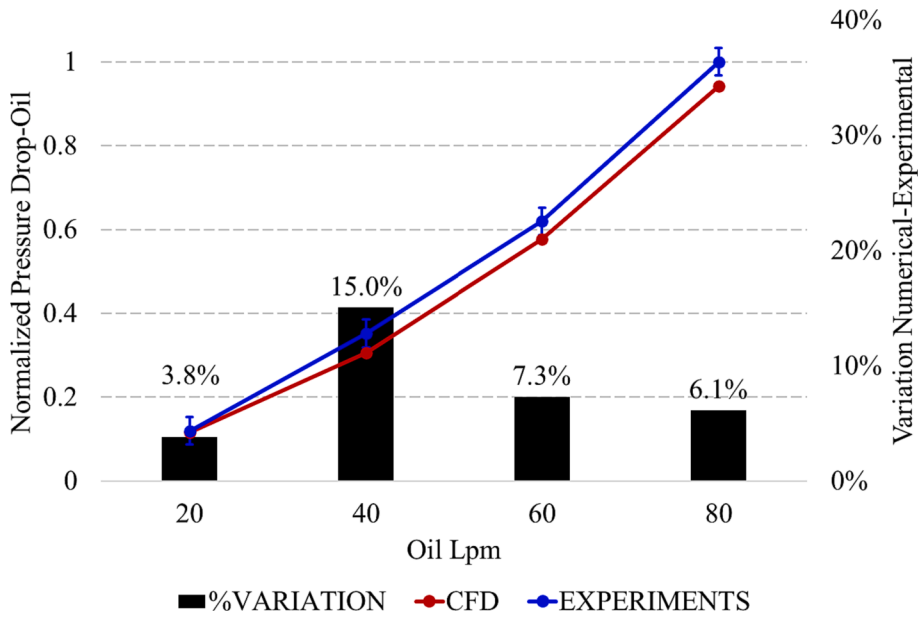

Fig. 20. Comparison between simulations and experiments in terms of normalized pressure drop of the oil circuit.

- $k-\varepsilon$ Realizable
- $k-\varepsilon$ Standard
- $k-\omega$ SST
- $k-\omega$ Standard
- RST- Elliptic Blending (EB)
- RST- Linear Pressure Strain (LPS)

Fig. 16 shows the results and the RST-LPS is the one giving the highest pressure drop (and sensibly higher than the one obtained with the $k-\omega$ SST model). For this reason, it is exploited to investigate the pressure drop of the entire exchanger with promising results able to match the experimental data, as it will be shown in the next paragraph. The results proposed in Fig. 16 are obtained with water but, qualitatively, the same is valid also for oil.

Apart from well-known models (such as the different versions of $k-\varepsilon$ and $k-\omega$) and the RST-LPS, the RST- Elliptic Blending (RST-EB) model is considered, which is an alternative to the RST-LPS. The RST-EB is a low Reynolds number model characterized by a function (based on a blending parameter which is a solution of an elliptic equation) that blends the formulation of the viscous sub-layer to the one of the log-layer for both the pressure strain and the dissipation terms. The model was proposed by Hanjalić *et al.* [43].

To highlight the difference between the models, the turbulent kinetic energy field is reported for each one in Fig. 17, over a section indicated in the same figure. It is worth to note that the $k-\omega$ variants show lower turbulent kinetic energy values, which are coherent with the predicted low values of pressure drop. $k-\varepsilon$ and RST models show similar distributions of k, with higher peaks with respect to the $k-\omega$ variants. In particular, the RST-LPS is the one that presents the highest peak value, once again in analogy to the pressure drop.

5.3. Heat transfer and pressure drop prediction

Four pairs of volumetric flow rates for coolant and oil have been selected to validate the proposed methodology both in terms of heat transfer and pressure drop. The time required for the simulation of a single operating condition is reported in Appendix A. The results show, with respect to the experimental data, a maximum relative error of 4.6 % for the heat transfer prediction, as visible in Fig. 18. The very limited errors underline the reliability of the proposed methodology, at least in terms of heat transfer.

Moving to the pressure drop, a comparison between numerical and experimental findings is proposed. In particular, Figs. 19 and 20 show results for water and oil, respectively.

First of all, even if not negligible, the errors are still acceptable, considering that with limited computational cost and time it is possible to estimate the pressure drop with an error lower than 15 %, which represent a useful information from a design standpoint. This is even more true considering that the alternative is represented by the simulation of the entire exchanger which requires unfeasible computational resources.

Moreover, it is necessary to point out that the major source of error is not related to the methodology (intended as ensemble of workflow and adopted numerical framework) proposed by the authors, rather it has to be ascribed to the turbulence model. As a demonstration of the methodology effectiveness, in Appendix B, a dedicated validation of the porous-medium-based approach (still on the investigated exchanger) is proposed.

As for the resulting temperature distributions inside the exchanger, some comments are proposed in the following. In Fig. 21a) and b), sections of the oil and water plates are visible. It is evident that both fluids undergo a non-negligible temperature gradient, which reflects into a non-negligible variation of the viscosity. This enforces the necessity to tune the porous model by means of the two-plate model, thus considering the effect of temperature gradient to properly estimate the pressure drop associated to each fluid.

In Fig. 22, the thermal field of the metal of the two-plate model is reported. In both the plates, the maximum temperature difference between the hottest and coldest points is nearly $15.5^{\circ}C$.

Furthermore, in Fig. 23 the effect of the application of periodic boundaries can be noticed. In particular, it is evident how the temperature peaks in the lower plate are in correspondence of the virtual contact with the turbulators of the upper plate. Simultaneously, this last shows a temperature drop at the virtual contact with the lower plate.

Before moving to the conclusions, it is important to point out that the proposed methodology is helpful (as an alternative to REV based approaches discussed in the introduction) to strongly reduce the computational effort in complex cases, where it is not possible to reduce the computational domain (for example exploiting symmetries) to calculate pressure drops and heat transfer. In other words, as in the currently investigated exchanger, the simulation of a single plate or even a slice of the exchanger is not able to ensure a reliable estimation of both the

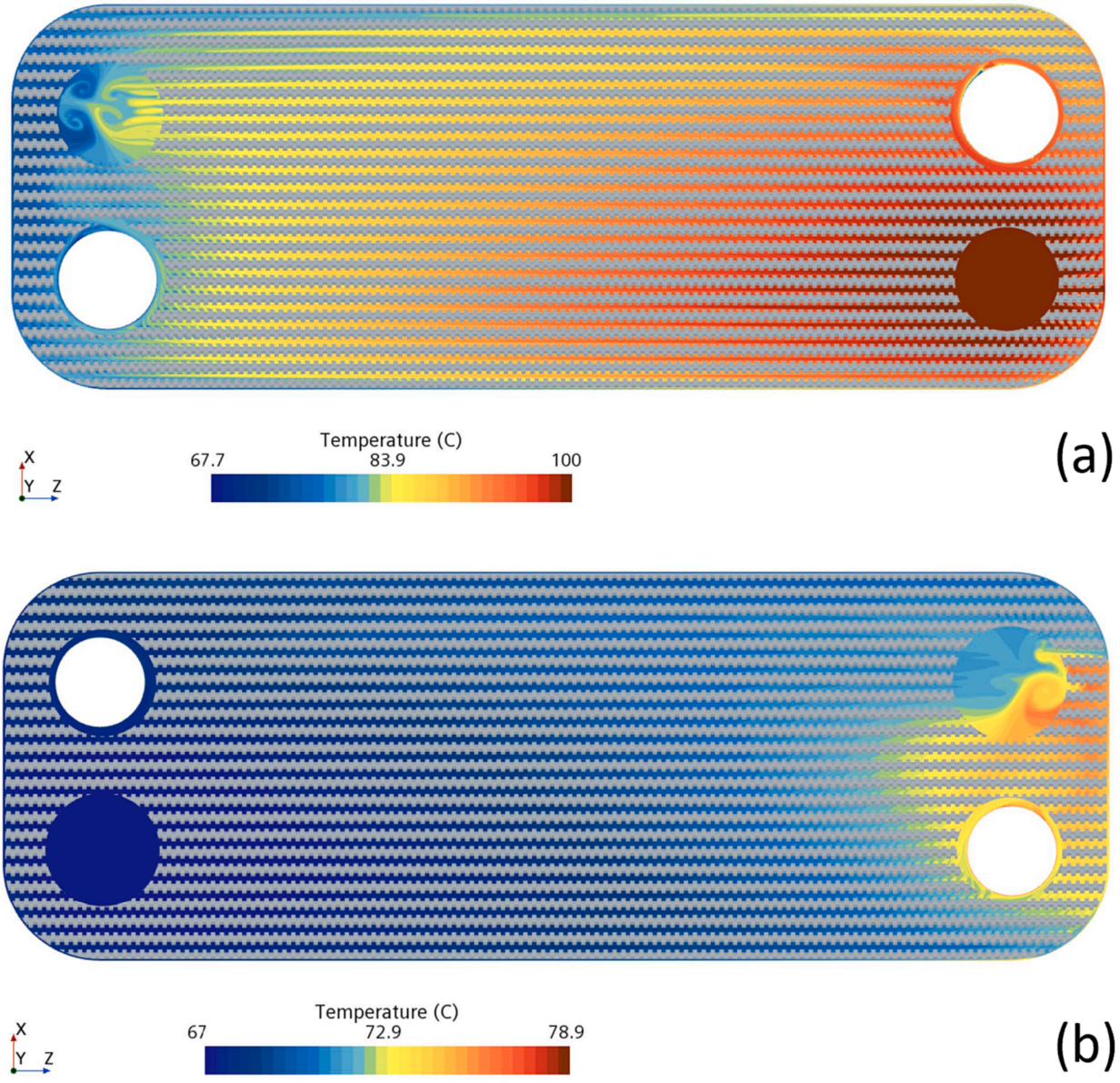

Fig. 21. Temperature fields over sections parallel to the plates are shown for the two-plate model. In (a), the temperature field of the oil in the middle of the oil-plate is reported, while (b) refers to the water plate.

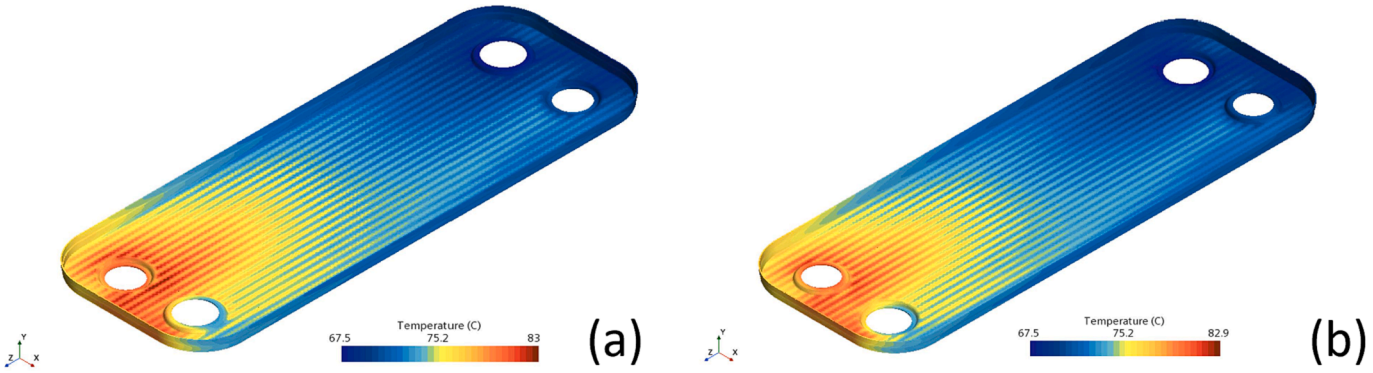

Fig. 22. Thermal field of the solid plates of the two-plate model. (a) Oil containing plate. (b) Water containing plate.

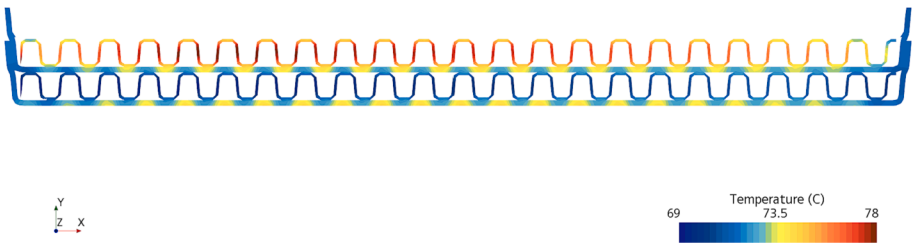

Fig. 23. Temperature field of the metal of plates and turbulators on the cross-section in the middle of the domain.

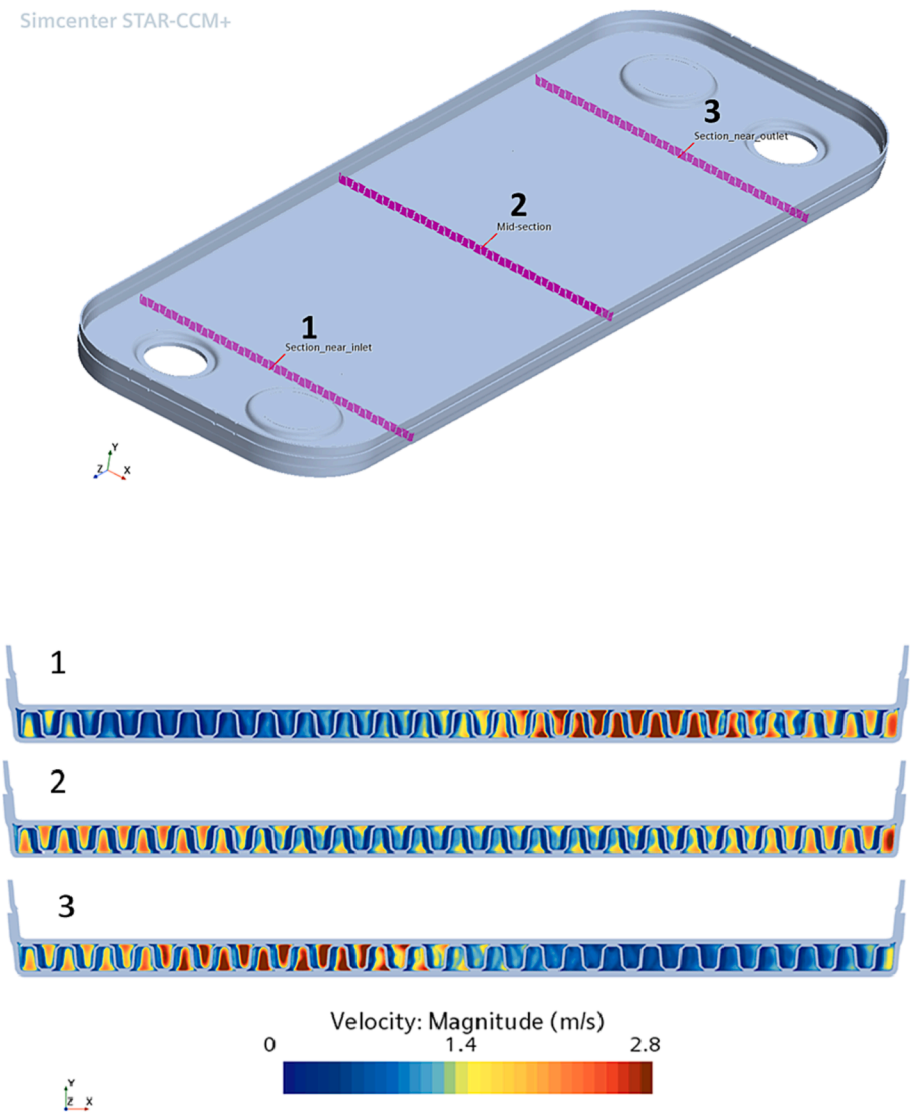

Fig. 24. Velocity field at three different sections of a plate of the water circuit: 1, 2 and 3 are close to inlet, mid-section and outlet, respectively.

losses across the fluid circuits and the heat transfer. In fact, the flow is strongly tridimensional, i.e. it is not uniformly distributed inside the plates and the mass flow rate is different plate-to-plate. In this regard, Fig. 24 shows the uneven flow inside a water plate (which is representative of all the plates of the investigated exchanger) along three different sections. Moreover, simulations reveal that the relative (i.e. plate-to-plate) variation of the mass flow rate registered on the porous model achieves 8 %. Since pressure drop variation with the flow rate (i.e. with the velocity) is super linear, investigating only a part of the domain under the hypothesis that the flow is uniformly distributed leads to wrong results. As for the heat transfer, the main issue in the simulation of a portion of the domain is related to the choice of the inlet temperatures of the two fluids, which are unknown.

6. Conclusions

A numerical methodology to perform 3D-CFD analyses of plate-fin heat exchangers is proposed, which overcomes the limit related to the computational cost, preventing the simulation of the whole device. As a matter of fact, the application of such a method allows to reduce of one order of magnitude the total number of cells required for the numerical grid of the entire exchanger, making the simulation feasible even

without extraordinary computational resources.

The methodology consists of different frameworks. Firstly, a Representative Elementary Volume is exploited to carry out a mesh sensitivity analysis which is mandatory to obtain a numerical grid that represents a compromise between accuracy and computational cost. Secondly, a two-plate exchanger (that is the original device but made of only two plates) characterized by periodic boundary conditions to mimic the presence of the adjacent plates is simulated to estimate the heat exchanged. Thirdly, the circuits of the two fluids are separately simulated to obtain the pressure drops. Such circuits are characterized by a simplified internal geometry, as turbulators are not present but modeled via a porous medium.

As for the numerical setup, the methodology relies on the Reynolds Stress Tensor turbulence model (specifically, the Linear Pressure Strain variant). In fact, compared to other investigated turbulence models, it provides the best estimation of pressure drops and heat transfer.

The robustness of the methodology is tested on a production plate-fin heat exchanger with turbulators (specifically an oil cooler for automotive application) by comparing the numerical results with the experimental ones. Four different operating conditions of the device are investigated, and, for all the cases, the error is at most 15 % for the pressure drops and lower than 4 % for the heat transfer estimations. Despite the errors are not negligible, they are still acceptable considering that the alternative is a computational domain consisting of hundred million cells. Moreover, it is demonstrated that the main reason for such errors has to be ascribed to the turbulence model and not to the proposed methodology.

CRediT authorship contribution statement

Federico Torri: Conceptualization, Data curation, Formal analysis, Investigation, Methodology, Software, Validation, Writing – original draft, Writing – review & editing. **Fabio Berni:** Conceptualization, Data curation, Formal analysis, Investigation, Methodology, Resources, Software, Supervision, Validation, Writing – original draft, Writing – review & editing. **Mauro Giacalone:** Formal analysis, Investigation, Software. **Sara Mantovani:** Conceptualization, Methodology, Supervision, Writing – original draft, Writing – review & editing. **Silvio Defanti:** Investigation, Methodology, Writing – original draft, Writing – review & editing. **Giulia Colombini:** Conceptualization, Methodology, Validation, Writing – original draft, Writing – review & editing. **Elena Bassoli:** Investigation, Resources, Supervision, Writing – original draft, Writing – review & editing. **Andrea Merulla:** Data curation, Funding acquisition, Investigation, Project administration, Resources, Supervision, Validation. **Stefano Fontanesi:** Conceptualization, Methodology, Supervision, Writing – original draft, Writing – review & editing.

Declaration of competing interest

The authors declare that they have no known competing financial interests or personal relationships that could have appeared to influence the work reported in this paper.

Data availability

The authors do not have permission to share data.

Acknowledgment

The authors gratefully acknowledge the University of Modena and Reggio Emilia for supporting the activity by the “Fondo di Ateneo per la Ricerca 2023 per il finanziamento di piani di sviluppo dipartimentale nell’ambito della ricerca” (FARD 2023) and the “Fondo di Ateneo per la Ricerca 2022 - Bando per il finanziamento di progetti dricerca interdisciplinari Mission Oriented – Linea FOMO” (FAR 2022).

Appendix A

The computational time required to perform the simulation of one operating point adopting the numerical frameworks shown in Fig. 6 is reported in Table 1:

Table 1
Computational time (in hour) of the methodology. Both the overall time and the one of each single framework are reported.

	[h]
REV x22	3.53
2 PLATES (PERIODIC)	88.69
SINGLE PLATE (POROUS) x2	0.08
MULTI PLATE (POROUS) x2	3
TOTAL	95.3

Each simulation is carried out with 64 cores (of a computer cluster), and it is stopped when an asymptotic stopping criterion is satisfied. The latter provides for 200 iterations in which the variations of pressure drop between inlet and outlet and overall heat transfer between the fluids (when present) are lower or equal than 1E-4 (in magnitude) between two consecutive iterations. Since there is no need to carry out a sensitivity to the turbulence model for each simulated heat exchanger, this time is not included in Table 1. Instead, the time needed for the mesh sensitivity is considered because the latter is required for each simulated device. It is useful to point out that, if the investigated operating conditions are not sensibly different, a mesh sensitivity just for one of the conditions is sufficient. Still on the computational time associated to the mesh sensitivity, it is calculated accounting for all the 22 simulations presented in the results in Paragraph 5.1 and required for the analysis of both the fluids. Similarly, the time for single and multi- plate simulations is accounted for twice, one for water and one for the oil.

Appendix B

In order to prove that the methodology based on the porous medium is robust (and the errors have to be ascribed to the turbulence model), a comparison is carried out with respect to the simulation of the whole exchanger. Since the latter cannot be entirely simulated with a proper mesh, the comparison is performed by means of a coarse grid. On the one hand, the adoption of such a grid allows the simulation of the whole exchanger but, on the other hand, it introduces a non-negligible numerical viscosity leading to non-negligible errors as shown in Paragraph 5.1. However, since the coarse mesh is exploited for both the entire device and the subsystem (reduced domain) utilized to calibrate the porous medium (which in turn is used

to model the entire device), the comparison is still fair. For brevity, only the water side is considered for the test. As for the mesh, apart from the core which moves from 0.15 mm to 0.4 mm, the prismatic near-wall grid is the same as the one adopted to obtain the results previously presented in Paragraph 5.1. It is important to point out that the simulations based on the porous medium are isothermal, but they have to account for the effect of the heat transfer on the pressure drop (related to the modification of the fluid properties) and, such effect, is included in the calibration of the porous medium constants. Even this aspect of the methodology (namely the inclusion of the heat transfer effect in the porous medium) requires validation. However, such a validation requires that the heat transfer is simulated in the model of the whole exchanger, i.e. that both the fluids are simultaneously present. In order to avoid a massive increase of the computational cost even in presence of coarse mesh, just water is accounted for, and walls are provided with a fixed and uniform temperature equal to the average between inlet and outlet temperatures of the oil. The investigated condition is one of the four analyzed in the main text, in particular it is the point with the highest flow rates. In the light of the previous observations, the adopted procedure can be resumed as follows:

I) The water pressure drop is measured on a single plate, characterized by actual geometry (visible in Fig 25 a)) and mesh coarser than the one selected for the analyses proposed in the main text of the paper (as visible from the comparison between the Figs. 25 b) and 25c)). The wall temperature is fixed to an average oil temperature between inlet and outlet, to allow heat transfer.

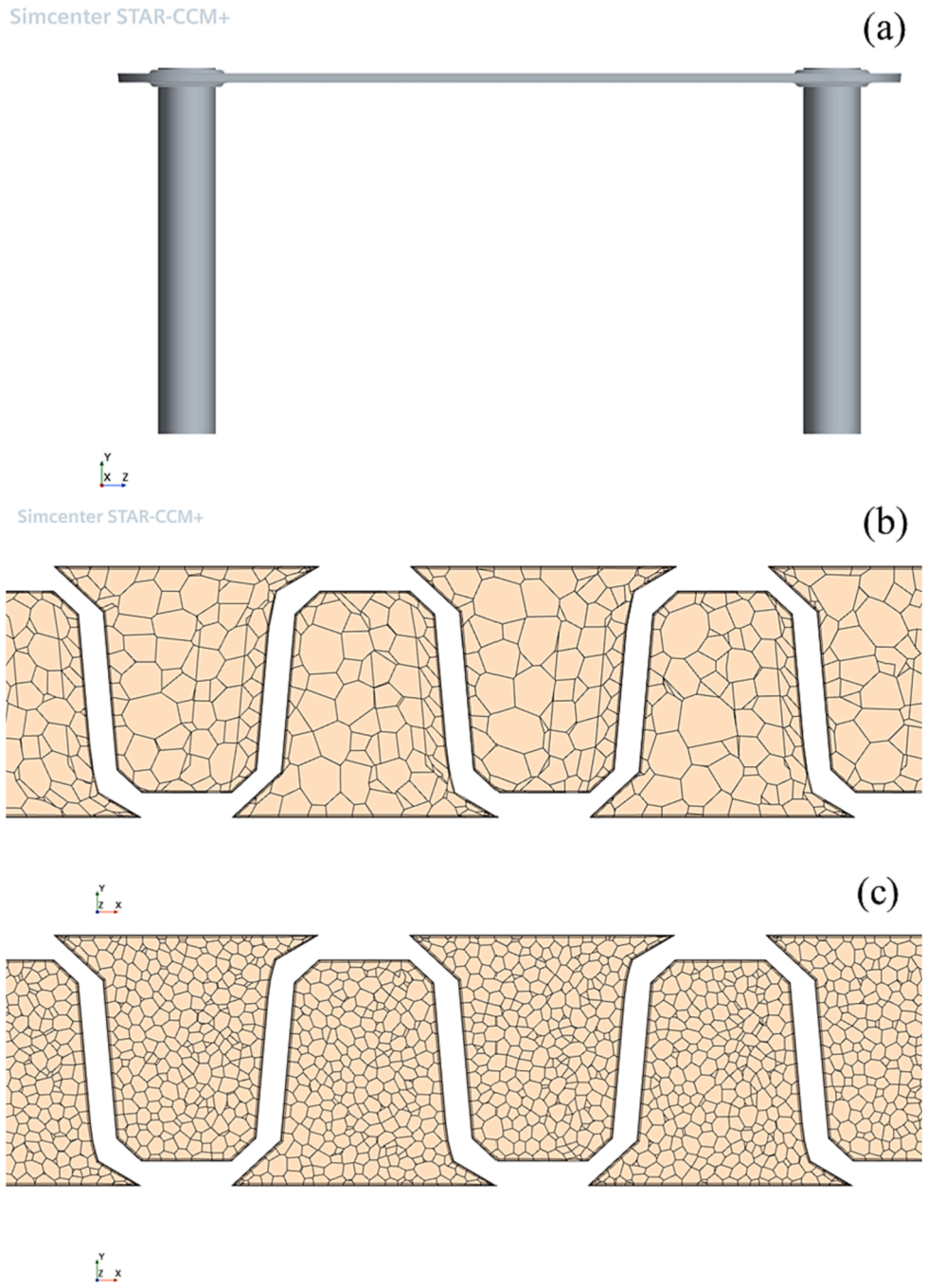

Fig. 25. (a) Single plate geometry, (b) Coarse Mesh (0.4 mm of cell dimension), (c) Fine Mesh (0.15 mm of cell dimension)

II) The entire water circuit shown in Fig. 10 and characterized by the actual geometry is simulated with the same coarse mesh. The wall temperature is the same as in the previous point.
III) A single plate with simplified geometry made of porous medium is then accounted for and it is visible in Fig. 12. The porous resistance of the latter is calibrated to match the pressure drop measured in the simulation of point I. The calculation is isothermal.
IV) The entire water circuit is simulated via the simplified geometry of Fig. 10 based on the porous medium calibrated at point III. The case is isothermal as well. The pressure drop across the circuit is measured and compared with the value obtained at point II.

The resulting difference between the simulations at points II and IV is negligible, as the "porous" circuit underestimates the pressure drop of the actual geometry of just 0.6 %. This is the evidence that the proposed methodology is reliable, and the main errors are due to the adopted turbulence model.

References

[1] R.K. Shah D.P. Sekulik, "FUNDAMENTALS OF HEAT EXCHANGER DESIGN," 2003. [Online]. Available: www.wiley.com.
[2] M.C. Georgiadis, S. Macchietto, Dynamic modelling and simulation of plate heat exchangers under milk fouling, Chem. Eng. Sci. 55 (9) (2000) 1605–1619, https://doi.org/10.1016/S0009-2509(99)00429-7.
[3] EPA, "Sources of Greenhouse Gas Emissions" 2023.
[4] EU, "EU measures against climate change" 2023.
[5] Y. Zhao, H. Cheng, Y. Wu, G. Zhu, "Exchanger Angle on the Performance of Plate Heat Numerical Simulation of Corrugated Inclination," 2014.
[6] O. Giurgiu, A. Pleşa, L. Socaciu, "Plate heat exchangers - flow analysis through mini channels", Energy Procedia Elsevier Ltd (2016) 244–251, https://doi.org/10.1016/j.egypro.2015.12.236.
[7] Y.N. Wang, et al., A study on 3D numerical model for plate heat exchanger, Procedia Eng., Elsevier Ltd (2017) 188–194, https://doi.org/10.1016/j.proeng.2017.01.203.
[8] A. Khanlari, A. Sözen, H.İ. Variyenli, Simulation and experimental analysis of heat transfer characteristics in the plate type heat exchangers using TiO2/water nanofluid, Int J Numer Methods Heat Fluid Flow 29 (4) (2019) 1343–1362, https://doi.org/10.1108/HFF-05-2018-0191.
[9] F. Afshari, A.D. Tuncer, A. Sözen, H.I. Variyenli, A. Khanlari, E.Y. Gürbüz, A comprehensive survey on utilization of hybrid nanofluid in plate heat exchanger with various number of plates, Int. J. Numer Methods Heat Fluid Flow 32 (1) (2022) 241–264, https://doi.org/10.1108/HFF-11-2020-0743.
[10] O. Arsenyeva, P. Kapustenko, L. Tovazhnyanskyy, G. Khavin, The influence of plate corrugations geometry on plate heat exchanger performance in specified process conditions, Energy 57 (2013) 201–207, https://doi.org/10.1016/j.energy.2012.12.034.
[11] M.J. Andrews, B.I. Master, Three-dimensional modeling of a helixchanger® heat exchanger using CFD, Heat Transfer Eng. 26 (6) (2005) 22–31, https://doi.org/10.1080/01457630590950871.
[12] A.G. Kanaris, A.A. Mouza, S.V. Paras, Flow and heat transfer prediction in a corrugated plate heat exchanger using a CFD code, Chem. Eng. Technol. 29 (8) (2006) 923–930, https://doi.org/10.1002/ceat.200600093.
[13] M. M. Aslam Bhutta, N. Hayat, M. H. Bashir, A. R. Khan, K. N. Ahmad, S. Khan, "CFD applications in various heat exchangers design: A review," *Applied Thermal Engineering*, 32 1. Elsevier Ltd, 1 12 2012 10.1016/j.applthermaleng.2011.09.001.
[14] Y. Menni, A. Azzi, A. Chamkha, "Enhancement of convective heat transfer in smooth air channels with wall-mounted obstacles in the flow path: A review," *Journal of Thermal Analysis and Calorimetry* 135 4. Springer Netherlands 1951 1976 28 2019 10.1007/s10973-018-7268-x.
[15] K. Sarraf, S. Launay, L. Tadrist, Complex 3D-flow analysis and corrugation angle effect in plate heat exchangers, Int. J. Therm. Sci. 94 (2015) 126–138, https://doi.org/10.1016/j.ijthermalsci.2015.03.002.
[16] C. Ranganayakulu, X. Luo, S. Kabelac, The single-blow transient testing technique for offset and wavy fins of compact plate-fin heat exchangers, Appl. Therm. Eng. 111 (2017) 1588–1595, https://doi.org/10.1016/j.applthermaleng.2016.05.118.
[17] D.B. Spalding, S.V. Patankar, Heat exchangers: design and theory sourcebook. a calculation procedure for the transient and steady-state behaviour of Shell-and-tube heat exchangers, 1st ed., McGraw Hill, 1972.
[18] D. Missirlis, et al., Numerical development of a heat transfer and pressure drop porosity model for a heat exchanger for aero engine applications, Appl. Therm. Eng. 30 (11–12) (2010) 1341–1350, https://doi.org/10.1016/j.applthermaleng.2010.02.021.
[19] D. Missirlis, K. Yakinthos, A. Palikaras, K. Katheder, A. Goulas, Experimental and numerical investigation of the flow field through a heat exchanger for aero-engine applications, Int. J. Heat Fluid Flow 26 (3) (2005) 440–458, https://doi.org/10.1016/j.ijheatfluidflow.2004.10.003.
[20] M. Musto, N. Bianco, G. Rotondo, F. Toscano, G. Pezzella, A simplified methodology to simulate a heat exchanger in an aircraft's oil cooler by means of a porous media model, Appl. Therm. Eng. 94 (2016) 836–845, https://doi.org/10.1016/j.applthermaleng.2015.10.147.
[21] M. C. Kauduinski Cardoso, D. Caldas, E. Fronza, L. H. Rodríguez Cisterna, M. Mortean, and M. Mantelli, *POROUS MEDIA APPROACH FOR HYDRODYNAMIC NUMERICAL SIMULATION OF COMPACT HEAT EXCHANGER*. 2020.
[22] W. Wang, J. Guo, S. Zhang, J. Yang, X. Ding, X. Zhan, Numerical study on hydrodynamic characteristics of plate-fin heat exchanger using porous media approach, Comput. Chem. Eng. 61 (2014) 30–37, https://doi.org/10.1016/j.compchemeng.2013.10.010.
[23] "MULTISCALE SIMULATIONS OF FLUID FLOW FOR FINNED ELLIPTIC TUBE HEAT EXCHANGERS USING POROUS MEDIA APPROACH," 2014. [Online]. Available: http://www.asme.org/about-asme/terms-of-use.
[24] Z. zhong Li, Y. dong Ding, Q. Liao, M. Cheng, X. Zhu, "An approach based on the porous media model for numerical simulation of 3D finned-tubes heat exchanger", Int. J. Heat Mass Transf 173 (2021) Jul, https://doi.org/10.1016/j.ijheatmasstransfer.2021.121226.
[25] A. Della Torre, G. Montenegro, A. Onorati, S. Khadilkar, R. Icarelli, Multi-scale CFD modeling of plate heat exchangers including offset-strip fins and dimple-type turbulators for automotive applications, Energies (basel) 12 (15) (2019), https://doi.org/10.3390/en12152965.
[26] D. Juan, Z. Hai-Tao, Numerical simulation of a plate-fin heat exchanger with offset fins using porous media approach, Heat Mass Transf. 54 (3) (2018) 745–755, https://doi.org/10.1007/s00231-017-2168-3.
[27] M. Yuan, P. Ming, W. Zhang, Numerical study of hydrodynamic and thermodynamic characteristics of a heat exchanger muffler, J. Mech. Sci. Technol. 33 (11) (2019) 5515–5525, https://doi.org/10.1007/s12206-019-1045-z.
[28] S. Mantovani, G.A. Campo, M. Giacalone, Steering column support topology optimization including lattice structure for metal additive manufacturing, Proc. Inst. Mech. Eng. C J. Mech. Eng. Sci 236 (21) (2020) 10645–10656, https://doi.org/10.1177/0954406220947121.
[29] E. Bassoli, S. Mantovani, M. Giacalone, A. Merulla, S. Defanti, On the technological feasibility of additively manufactured self-supporting AlSi10Mg lattice structures, Adv. Eng. Mater 25 (3) (2023) 2201074, https://doi.org/10.1002/adem.202201074.
[30] W. Chang, G. Pu-Zhen, T. Si-Chao, X. Chao, Effect of aspect ratio on the laminar-to-turbulent transition in rectangular channel, Ann. Nucl. Energy 46 (2012) 90–96, https://doi.org/10.1016/j.anucene.2012.03.018.
[31] S.G. Kandlikar, M.R. King, in: "chapter 1 - Introduction", in Heat Transfer and Fluid Flow in Minichannels and Microchannels (second Edition), Butterworth-Heinemann, Oxford, 2014, pp. 1–9, https://doi.org/10.1016/B978-0-08-098346-2.00001-6.
[32] Siemens Digital Industries Software. Siemens STAR-CCM++ User Guide, 2023.
[33] M.M. Gibson, B.E. Launder, Ground effects on pressure fluctuations in the atmospheric boundary layer, J. Fluid Mech. 86 (3) (1978) 491–511, https://doi.org/10.1017/S0022112078001251.
[34] B.E. Launder, N. Shima, Second-moment closure for the near-wall sublayer - development and application, AIAA J. 27 (10) (1989) 1319–1325, https://doi.org/10.2514/3.10267.
[35] B.E. Launder, G.J. Reece, W. Rodi, Progress in the development of a Reynolds-stress turbulence closure, J Fluid Mech 68 (3) (1975) 537–566, https://doi.org/10.1017/S0022112075001814.
[36] T.J. Craft, B.E. Launder, New wall-reflection model applied to the turbulent impinging jet, AIAA J. 30 (12) (1992) 2970–2972, https://doi.org/10.2514/3.48980.
[37] D. Wilcox, *Turbulence Modeling for CFD (Third Edition) (Hardcover)*. 2006.
[38] W. Rodi, Experience with two-layer models combining the k-epsilon model with a one-equation model near the wall, American Institute of Aeronautics and Astronautics (AIAA) (1991), https://doi.org/10.2514/6.1991-216.
[39] M. Wolfshtein, The velocity and temperature distribution in one-dimensional flow with turbulence augmentation and pressure gradient, Int J Heat Mass Transf. 12 (3) (1969) 301–318, https://doi.org/10.1016/0017-9310(69)90012-X.
[40] T. Jongen, "Simulation and modeling of turbulent incompressible fluid flows." doi: 10.5075/epfl-thesis-1758.
[41] F. Torri, et al., Evaluation of TPMS Structures for the Design of High Performance Heat Exchangers, SAE Technical Paper Series (2023) (Online).
[42] I.A. Stogiannis, S.V. Paras, O.P. Arsenyeva, P.O. Kapustenko, "CFD modelling of hydrodynamics and heat transfer in channels of a PHE", Chem. Eng. Transactions Italian Association of Chemical Eng - AIDIC (2013) 1285–1290, https://doi.org/10.3303/CET1335214.
[43] R. Manceau, K. Hanjalić, Elliptic blending model: a new near-wall reynolds-stress turbulence closure, Phys. Fluids 14 (2) (2002) 744–754, https://doi.org/10.1063/1.1432693.